

An Analysis of Infrared and Visible Atmospheric Extinction Measurements In Europe

Janet E. Shields

Approved for public release; distribution unlimited.

Scientific Report No. 18
June 1981

Contract No. F19628-78-C-0200
Project No. 7670
Task No. 7670-14
Work Unit No. 7670-14-01

Contract Monitor, Major John D. Mill, USAF
Optical Physics Division

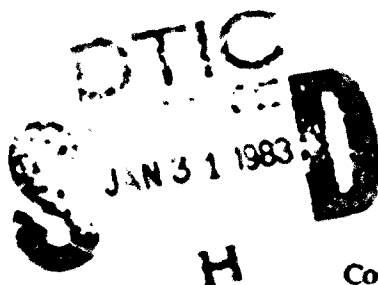
Prepared for
Air Force Geophysics Laboratory, Air Force Systems Command
United States Air Force, Hanscom AFB, Massachusetts 01731

VISIBILITY LABORATORY La Jolla, California 92093

UNIVERSITY
OF
CALIFORNIA
SAN DIEGO



SCRIPPS
INSTITUTION
OF
OCEANOGRAPHY



DA 123 999

DTIC FILE COPY

83 01 31 057

UNCLASSIFIED

SECURITY CLASSIFICATION OF THIS PAGE (When Data Entered)

REPORT DOCUMENTATION PAGE		READ INSTRUCTIONS BEFORE COMPLETING FORM
1. REPORT NUMBER AFGL-TR-81-0251	2. GOVT ACCESSION NO. AD-A123 999	3. RECIPIENT'S CATALOG NUMBER
4. TITLE (and Subtitle) AN ANALYSIS OF INFRARED AND VISIBLE ATMOSPHERIC EXTINCTION MEASUREMENTS IN EUROPE		5. TYPE OF REPORT & PERIOD COVERED Scientific - Interim Scientific Report No. 18
		6. PERFORMING ORG. REPORT NUMBER SIO Ref. 82-4
7. AUTHOR(s) Janet E. Shields		8. CONTRACT OR GRANT NUMBER(s) F19628-78-C-0200
9. PERFORMING ORGANIZATION NAME AND ADDRESS University of California, San Diego Visibility Laboratory La Jolla, California 92093		10. PROGRAM ELEMENT, PROJECT, TASK AREA & WORK UNIT NUMBERS 62101F 7670-14-01
11. CONTROLLING OFFICE NAME AND ADDRESS Air Force Geophysics Laboratory Hanscom AFB, Massachusetts 01731 Contract Monitor: Major John D. Mill/OPA		12. REPORT DATE June 1981
		13. NUMBER OF PAGES 34
14. MONITORING AGENCY NAME & ADDRESS (if different from Controlling Office)		15. SECURITY CLASS. (of this report) UNCLASSIFIED
		15a. DECLASSIFICATION/DOWNGRADING SCHEDULE
16. DISTRIBUTION STATEMENT (of this Report) Approved for public release; distribution unlimited.		
17. DISTRIBUTION STATEMENT (of the abstract entered in Block 20, if different from Report)		
18. SUPPLEMENTARY NOTES		
19. KEY WORDS (Continue on reverse side if necessary and identify by block number) <div style="display: flex; justify-content: space-between;"> <div> Aerosol Extinction Coefficient Atmospheric Aerosols Atmospheric Optical Properties </div> <div> Atmospheric Extinction Coefficient Infrared Extinction Infrared Transmittance </div> </div>		
20. ABSTRACT (Continue on reverse side if necessary and identify by block number) This report contains an analysis of simultaneous ground-based measurements of infrared (3-5 μ m and 8-12 μ m) and visible (photopic) atmospheric extinction. The measurements were taken at hourly intervals over three 3-month periods in the Netherlands, as part of the NATO OPAQUE program. The measurements were made by the Physics Group of the Physics Laboratory of the National Defense Research Organization-TNO, at Ypenberg Air Base, Netherlands. The analysis is based on preliminary data.		

DD FORM 1473
1 JAN 73EDITION OF 1 NOV 68 IS OBSOLETE
S/N 0102-014-6601

UNCLASSIFIED

SECURITY CLASSIFICATION OF THIS PAGE (When Data Entered)

20. ABSTRACT continued:

A scheme for sorting the infrared aerosol particle extinctions was devised, taking into consideration the form of the observed parameter relationships, the expected measurement uncertainty, and the theoretically predicted conditions associated with high infrared aerosol extinction. The data were sorted into an upper bin, consisting primarily of mist to fog cases, and a lower bin, consisting primarily of clear to haze cases. Here "mist" is defined as a suspension of water droplets or wet hygroscopic particles (not a drizzle) causing reduced visibility greater than 1 km. When the visibility is reduced in this manner to 1 km or less, the condition is defined to be fog.

The upper (mist) bin, defined as those points with visual extinction coefficient greater than 1 km^{-1} (visibility less than 5 km) and relative humidity of 94% or greater, included essentially all of the high infrared aerosol extinction values. Using both visual extinction and relative humidity thresholds, rather than either threshold alone, yielded much more effective sorting of the infrared extinctions. These thresholds are based on the preliminary data release. Relative humidities near 94% have been corrected to near 99% in edited versions of the data base, released after this report was written.

In the lower bin (haze) category, the infrared aerosol extinction (due to aerosol particle scattering and absorption) was consistently low relative to the extinction caused by air molecule scattering and absorption and water vapor absorption. The aerosol extinction in the $3\text{-}5\mu\text{m}$ and $8\text{-}12\mu\text{m}$ regions averaged near $.02 \text{ km}^{-1}$ in the summer and $.01 \text{ km}^{-1}$ in the winter. These values compare reasonably with LOWTRAN model estimates. Thus for these conditions, *i.e.* visual extinction of 1 km^{-1} or less or relative humidity less than 94%, the aerosol extinction was consistently low.

In the upper bin (mist) category, the infrared aerosol particle extinction was found to vary over a wide range, with a median extinction of about $.1 \text{ km}^{-1}$ and with a significant number of extinctions of 1 to 10 km^{-1} or higher. The aerosol extinctions exceeded the air molecule and water vapor extinction only about 20% of the time and exceeded 1 km^{-1} only about 10% of the time. These high extinctions, occurring 10-20% of the time, compare well with the LOWTRAN fog models. The incidence of the high extinctions was distributed over the whole range of visual extinction in the mist bin, and persistence calculations indicate that the infrared aerosol extinctions have low persistence relative to the visual extinction and relative to the duration of the mist episodes.

Thus for this upper bin (mist) category, the infrared aerosol extinction reaches significantly high magnitudes less often than expected, and persists only over short time intervals. Measurements in addition to visible extinction coefficient and relative humidity would be required to predict the incidence of high infrared extinction within mist episodes. In the absence of this information one can still make statistical estimates of occurrence probabilities using cumulative frequency distributions of the infrared to visible aerosol extinction ratio.

**AN ANALYSIS OF INFRARED AND VISIBLE
ATMOSPHERIC EXTINCTION MEASUREMENTS IN EUROPE**

Janet E. Shields

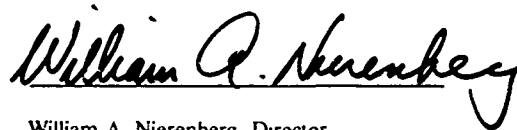
Visibility Laboratory
University of California, San Diego
Scripps Institution of Oceanography
La Jolla, California 92093

Approved:



Roswell W. Austin, Director
Visibility Laboratory

Approved:



William A. Nierenberg, Director
Scripps Institution of Oceanography

CONTRACT NO. F19628-78-C-0200

Project No. 7670

Task No. 7670-14

Work Unit No. 7670-14-01

Scientific Report No. 18

June 1981

Contract Monitor

Major John D. Mill, Atmospheric Optics Branch, Optical Physics Division

Approved for public release; distribution unlimited.

Prepared for

**AIR FORCE GEOPHYSICS LABORATORY
AIR FORCE SYSTEMS COMMAND
UNITED STATES AIR FORCE
HANSCOM AFB, MASSACHUSETTS 01731**

SUMMARY

This report contains an analysis of simultaneous ground-based measurements of infrared (3-5 μ m and 8-12 μ m) and visible (photopic) atmospheric extinction. The measurements were taken at hourly intervals over three 3-month periods in the Netherlands, as part of the NATO OPAQUE program. The measurements were made by the Physics Group of the Physics Laboratory of the National Defense Research Organization-TNO, at Ypenberg Air Base, Netherlands. The analysis is based on preliminary data.

A scheme for sorting the infrared aerosol particle extinctions was devised, taking into consideration the form of the observed parameter relationships, the expected measurement uncertainty, and the theoretically predicted conditions associated with high infrared aerosol extinction. The data were sorted into an upper bin, consisting primarily of mist to fog cases, and a lower bin, consisting primarily of clear to haze cases. Here "mist" is defined as a suspension of water droplets or wet hygroscopic particles (not a drizzle) causing reduced visibility greater than 1 km. When the visibility is reduced in this manner to 1 km or less, the condition is defined to be fog.

The upper (mist) bin, defined as those points with visual extinction coefficient greater than 1 km⁻¹ (visibility less than 3 km) and relative humidity of 94% or greater, included essentially all of the high infrared aerosol extinction values. Using both visual extinction and relative humidity thresholds, rather than either threshold alone, yielded much more effective sorting of the infrared extinctions. These thresholds are based on the preliminary data release. Relative humidities near 94% have been corrected to near 99% in edited versions of the data base, released after this report was written.

In the lower bin (haze) category, the infrared aerosol extinction (due to aerosol particle scattering and absorption) was consistently low relative to the extinction caused by air molecule scattering and absorption and water vapor absorption. The aerosol extinction in the 3-5 μ m and 8-12 μ m regions averaged near .02 km⁻¹ in the summer and .01 km⁻¹ in the winter. These values compare reasonably with LOWTRAN model estimates. Thus for these conditions, i.e. visual extinction of 1 km⁻¹ or less or relative humidity less than 94%, the aerosol extinction was consistently low.

In the upper bin (mist) category, the infrared aerosol particle extinction was found to vary over a wide range, with a median extinction of about .1 km⁻¹ and with a significant number of extinctions of 1 to 10 km⁻¹ or higher. The aerosol extinctions exceeded the air molecule and water vapor extinction only about 20% of the time and exceeded 1 km⁻¹ only about 10% of the time. These high extinctions, occurring 10-20% of the time, compare well with the LOWTRAN fog models. The incidence of the high extinctions was distributed over the whole range of visual extinction in the mist bin, and persistence calculations indicate that the infrared aerosol extinctions have low persistence relative to the visual extinction and relative to the duration of the mist episodes.

Thus for this upper bin (mist) category, the infrared aerosol extinction reaches significantly high magnitudes less often than expected, and persists only over short time intervals. Measurements in addition to visible extinction coefficient and relative humidity would be required to predict the incidence of high infrared extinction within mist episodes. In the absence of this information one can still make statistical estimates of occurrence probabilities using cumulative frequency distributions of the infrared to visible aerosol extinction ratio.



Accession For	NTIS GRA&I	<input checked="" type="checkbox"/>	<input type="checkbox"/>
	DTIC TAB		
	Unannounced		
	Justification		
By	Distribution/		
	Availability Codes		
Dist	Avail and/or		
	Special		

TABLE OF CONTENTS

SUMMARY	v
LIST OF TABLES AND ILLUSTRATIONS	ix
1. INTRODUCTION	1
1.1 Goals of the Analysis	1
2. THEORY AND BACKGROUND	1
2.1 Definition of Terms	1
2.2 Related Theoretical Studies	2
3. DISCUSSION OF THE MEASUREMENTS	3
3.1 The OPAQUE Program	3
3.2 Instrument Discussion--Visible	4
3.3 Instrument Discussion--Infrared	4
4. DATA REDUCTION	5
4.1 Derivation of Aerosol Extinction Coefficients	5
5. DATA ANALYSIS--DEVELOPMENT OF THE BIN CONCEPT	6
5.1 General Parameter Relationships	6
5.2 Infrared Aerosol Extinction Uncertainties	7
5.3 Method to Sort Infrared Extinctions	10
5.4 Results of Sorting the Data	11
5.5 Application of the Sorting Mechanism to Other Seasons	12
6. DATA ANALYSIS--CHARACTERISTICS OF THE BINS	12
6.1 Characteristics of the Lower Bin	12
6.2 Estimation of Infrared Extinction for Haze Cases	14
6.3 Comparison of Measured and Model Haze Aerosol Extinctions	15
6.4 Summary for Lower Bin (Haze) Cases	16

6.5 Characteristics of the Upper Bin	16
6.6 Study of the IR Aerosol Extinction Persistence in the Upper Bin	18
6.7 Estimation of Infrared Extinction for Mist and Fog Cases	21
6.8 Comparison of Measured and Model Mist and Fog Aerosol Extinctions	21
6.9 Summary for Upper Bin (Mist) Cases	23
 7. SUGGESTED FURTHER WORK TO ENHANCE THE ANALYSIS	 23
7.1 Analysis of the OPAQUE Data	23
7.2 Further Experimental Work	23
 8. CONCLUSION	 24
 9. REFERENCES	 25
 10. ACKNOWLEDGEMENTS	 26
 APPENDIX A: Visibility Laboratory Contracts & Related Publications	 26
 APPENDIX B: Analytic Update	 27
 APPENDIX C: Further Comments on Infrared Aerosol Extinction Uncertainties	 27

LIST OF TABLES AND ILLUSTRATIONS

Table No.		Page
3.1	Measured Variables Used for Analysis	4
4.1	Constants for Molecular Transmittance Computation	5
5.1	Aerosol Extinction Uncertainty	8
5.2	Bin Statistics, Aerosol Extinction (3-5 μm)	12
5.3	Bin Statistics, Aerosol Extinction (8-12 μm)	12
6.1	Observed Variation and Measurement Uncertainty, Lower Bin	14
6.2	Cumulative Frequency, Aerosol Extinction, Lower Bin	14
6.3	Measured and Modelled Aerosol Extinctions Lower Bin	16
6.4	Aerosol Extinction Values in Upper Bin	17
6.5	Squared Persistence Correlation Coefficient, Upper Bin	19
6.6	Related Persistence Statistics, Upper Bin	20
6.7	Cumulative Frequency of Extinction Ratio, Upper Bin	21
6.8	Measured Extinction Ratios, Upper Bin	21
6.9	LOWTRAN5 Extinction Ratios	21

Fig. No.		Page
3-1	Map of Netherlands OPAQUE Station Location	3
5-1	Infrared Aerosol Extinction vs Visible Scattering Coefficient	6
5-2	Infrared Aerosol Extinction vs Relative Humidity	7
5-3	Visible Scattering Coefficient vs Relative Humidity	7
5-4	Uncertainty in Infrared Aerosol Extinction	8
5-5	Final vs Beginning Aerosol Extinction	9
5-6	Visible Scattering and Relative Humidity Thresholds for Bins	10
5-7	Histogram of Aerosol Extinction	11
5-8	Cumulative Frequency of Aerosol Extinction	13
6-1	Cumulative Frequency of Estimate Error ² Lower Bin	15
6-2	Measured and Model Aerosol Extinctions, Lower Bin	16
6-3	Histogram of Extinction Ratio (IR/Vis), Upper Bin	17
6-4	Extinction Ratio (IR/Vis) vs Visible Scattering, Upper Bin	18
6-5	Persistence Correlation Coefficient for Upper Bin	19
6-6	Extinction Variations Within a Mist Episode	20
6-7	Cumulative Frequency of Estimate Error ² Upper Bin	22
6-8	Measured and Model Extinction Ratios, Upper Bin	23

An Analysis of Infrared and Visible Atmospheric Extinction Measurements in Europe

Janet E. Shields

1. INTRODUCTION

As electro-optical systems are used for a growing variety of applications, there is an increasing requirement for understanding and predicting the atmospheric influences on system performance. In support of this requirement, the Visibility Laboratory has maintained an extensive program of visible optical and meteorological measurements and has been involved in the analysis of data taken under the NATO program OPAQUE (Optical Atmospheric Quantities in Europe), documented in Fenn (1978). The OPAQUE program consisted primarily of a series of ground-based optical measurements taken in the visible and infrared portions of the spectrum, along with approximately simultaneous meteorological measurements. These measurements were recorded at several stations throughout Europe at hourly intervals over a two year period. This report deals with an analysis of some of the infrared data taken during Project OPAQUE.

There are a variety of optical infrared sensors in use today, whose performance is partly dependent on the atmospheric infrared extinction. Mie calculations based on model particle size distributions result in the following trends [Shettle and Fenn (1979)]. When the atmospheric conditions range from clear to hazy, aerosol extinctions are generally smaller at infrared wavelengths than at visible wavelengths. Except in very clear air, this will result in better optical propagation within the infrared "window" regions (about $3\text{-}5\mu\text{m}$ and $8\text{-}13\mu\text{m}$) than at visible wavelengths. However in the presence of large droplets of size about equal to the wavelength, such as may occur in mist and fog, the infrared aerosol extinction can become greater than the visible aerosol extinction, resulting in poorer optical propagation of infrared wavelengths.

Unlike the visible extinction, the infrared extinction is difficult and expensive to measure. Additionally, the infrared extinction is difficult to estimate from visible measurements, since the infrared to visible extinction relationship is influenced by the aerosol particle size distribution and index of refraction, which are also difficult to measure. As a result, there is interest in evaluating how well present models estimate the infrared extinction and in developing improved empirical means of estimating the infrared extinction.

1.1 Goals of the Analysis

This analysis of the OPAQUE data was directed toward two goals. The first goal was to evaluate the variations in the measured data relative to model predictions. In general, haziness and the associated optical changes, such as a decrease in the radiance transmittance, are caused by increases in the aerosol particle content of the atmosphere. This aerosol includes droplets which may be composed of varying fractions of water, sea salt, soot, and so on, as well as solid particles such as dust. Measurements have been made of the size distribution of these particles, their chemical content, and their indices of refraction. Most models are based on Mie calculations whose inputs are the most likely aerosol particle size distributions and the most likely refractive index distributions as a function of wavelength. Since measured aerosol characteristics in the atmosphere vary, it is to be expected that the transmittance also should vary. The extensive OPAQUE data set, which clearly illustrates these typical radiance transmittance variations, should be valuable for evaluating how well the models predict them.

The second goal of the analysis was to develop improved techniques for estimating the infrared transmittance based on more conventional measurements and observations. Like the infrared transmittance, the visible transmittance is also influenced by the aerosols. The meteorological quantities are also related to the aerosols. For example, aerosol particle size is influenced by relative humidity, and aerosol content is influenced by airmass history. Since the visible, meteorological, and infrared regimes affect or are affected by the aerosols, it might be possible to develop an adequate empirical model to relate the infrared radiance transmittance directly to the visible and meteorological quantities.

2. THEORY AND BACKGROUND

2.1 Definition of Terms

In this analysis, the parameter of interest is the radiance transmittance in the infrared. The transmittance, which is a function of path length, is defined at wavelength λ as the proportion of the incident beam which remains after traveling over a given path.

$$T_{\lambda}(r) = N_{\lambda}(r)/N_{\lambda}(0), \quad (2-1)$$

where $N_{\lambda}(r)$ and $N_{\lambda}(0)$ are the radiances at wavelength λ and path lengths r and 0. Equation (2-1) is correct for monochromatic radiation. Broadband sensors, such as those utilized during Project OPAQUE, measure a weighted transmittance,

$$\bar{T} = \frac{\int_{\lambda} T_{\lambda} N_{\lambda} R_{\lambda} d\lambda}{\int_{\lambda} N_{\lambda} R_{\lambda} d\lambda}, \quad (2-2)$$

where N_{λ} is the radiance of the source (in this case a 650° blackbody) and R_{λ} is the spectral response of the sensor.

The monochromatic transmittance at wavelength λ may also be defined in terms of the monochromatic extinction coefficient α_{λ} ,

$$T_{\lambda} = e^{-\alpha_{\lambda} r}. \quad (2-3)$$

The effective broadband extinction coefficient is defined by either of two non-equivalent definitions depending on the application. For direct broadband measurements of absorption and scattering, the instrument response depends on an effective extinction coefficient defined by

$$\bar{\alpha}_1 = \frac{\int_{\lambda} \alpha_{\lambda} N_{\lambda} R_{\lambda} d\lambda}{\int_{\lambda} N_{\lambda} R_{\lambda} d\lambda}. \quad (2-4)$$

However for direct broadband measurements of transmittance or transmitted light, the instrument response depends on an effective extinction coefficient defined by

$$\bar{\alpha}_2 = \frac{-\ln \bar{T}}{r} \quad (2-5)$$

(with \bar{T} defined in Eq. 2-2), which may be range dependent. This range dependence occurs when the attenuation is wavelength selective within the band, because the spectral content of the light is in that case range dependent. In the case of aerosol extinction, the range dependence is very slight, and Eqs. (2-4) and (2-5) are nearly equivalent.

The transmittance may be represented as the product of three components,

$$T = T_{aer} \cdot T_{H_2O}(r, T_d) \cdot T_{Mol}(r). \quad (2-6)$$

T_{aer} is the transmittance due to the aerosol particles, i.e. the wet and dry particles in the atmosphere. T_{H_2O} is the transmittance due to molecular water vapor. It is a function of temperature and dewpoint temperature or water

vapor. T_{Mol} is the transmittance due to the air molecule components, such as carbon dioxide. It is a function of temperature. (For convenience, these transmittances and the associated extinction coefficients will be designated by the adjectives "aerosol", "water vapor", and "molecular".) All of these components include both scattering and absorption. Although Eq. (2-6) is strictly correct only for monochromatic radiance, treating each of the components as an integral analogous to Eq. (2-2) results in errors to the total transmittance which are usually less than 1% in the window regions. [Shettle (1978a)].

Most of the uncertainty in the estimation of infrared transmittance from model inputs is due to the uncertainty in estimating the aerosol attenuation. The general consensus [Nilsson (1979) and Roberts (1976)] seems to be that given measurements of temperature and humidity, the water vapor and molecular extinctions are well handled by computer programs, such as LOWTRAN 5 [Kneizys *et al.* (1980)]. This analysis deals with the aerosol transmittance and the associated aerosol extinction.

2.2 Related Theoretical Studies

There has been a great deal of work on the various theoretical aspects of predicting aerosol particle extinction. Two rather well thought out works are those of Shettle and Fenn (1979) and Nilsson (1979). These papers discuss the most probable aerosol characteristics such as particle size, and show the resulting computed extinction characteristics. Pinnick *et al.* (1979) report similar calculations based on the measured drop size properties of fogs.

In general, the results of these calculations may be summarized as follows. If the relative particle size distribution and refractive index distribution of the aerosol remain constant, and only the number density changes, then the magnitude of the aerosol extinction coefficient will vary, but the spectral relationships will be fixed. That is, the ratio of extinction coefficient at two given wavelengths will be a constant. If relative particle size distribution or refractive index distribution are allowed to change, then the spectral relationships will change.

The visible extinction should be more strongly affected by the sub-micron region of the particle size distribution, while the infrared extinction should be more strongly affected by the larger particles in the micron region of the particle size distribution [as may be inferred from figures in Nilsson (1979)]. The terms accumulation and coarse modes [Whitby (1978)] refer to two peaks often observed at two size ranges in the particle size distribution. Since these size ranges are partly influenced by independent processes, the two modes may not always be closely related [Fitch and Cress (1981) and Whitby (1978)]. Thus one might expect some variation in the visible to infrared extinction relationship. Jennings *et al.* (1978) discuss the effect of refractive index variations on atmospheric extinction.

One difficulty inherent in the aerosol extinction calculations is the difficulty in assigning reasonable particle size distributions. The distributions respond to a number

of environmental factors, both macroscopic and microscopic. For example, Yue and Deepak (1980) discuss the effects of sedimentation rates on the drop size distribution in fogs.

In spite of the uncertainties in particle size distribution and refractive index, models based on particle size distributions can be very useful. Perhaps the most commonly used model of this sort is the LOWTRAN model. LOWTRAN essentially uses four haze models and two fog models for the aerosol portion of the program. The haze models are based on an assignment of the most likely particle size distribution and refractive index distribution for four conditions: urban, rural, maritime, and tropospheric. In the LOWTRAN 3B model, the relative particle size distribution and refractive index distribution are held constant within each model, and only the number density is allowed to vary. Thus, for a given model, say rural, the ratio of extinction coefficient at two given wavelengths is a constant.

In the LOWTRAN 5 model [Kneizys *et al.* (1980)] the effect of relative humidity on relative particle size distribution and refractive index is included. Thus the ratio of infrared to visible aerosol extinction coefficient is no longer a constant, but is a function of relative humidity. The effect of relative humidity is much stronger in the maritime model than in the urban or rural models. The analysis in this report will include some discussion of how the measured infrared to visible ratios compare with the ratios inherent in the LOWTRAN models.

3. DISCUSSION OF THE MEASUREMENTS

3.1 The OPAQUE Program

The OPAQUE program was an extensive measurement program undertaken by several nations connected through NATO. Measurements were taken at hourly intervals over a two year period at several stations throughout Europe. The program is well documented in Fenn (1978). The analysis leading up to this report was begun using a small set of data [Johnson, *et al.* (1979b)], and then expanded to include larger portions of the data base. Portions of the Netherlands data set were chosen for analysis because the Netherlands data appeared to be the most complete and self consistent set available at the time. The present report is based upon 9 months of Netherlands preliminary release data. (See Appendix B.)

The measurements were made by the Physics Group of the Physics Laboratory of the National Defense Research Organization-TNO, at Ypenberg Air Base [Janssen (1981)]. The Netherlands OPAQUE station is located at the Royal Air Force Base Ypenburg, near The Hague and Rotterdam. It is near the coast, but is influenced by the urban industrial environment [Fenn (1978)]. Figure 3-1 illustrates the location of the Netherlands OPAQUE station.

The OPAQUE program included measurements of visible extinction coefficient, horizontal and vertical illuminance, path radiance, infrared transmittance, optical and

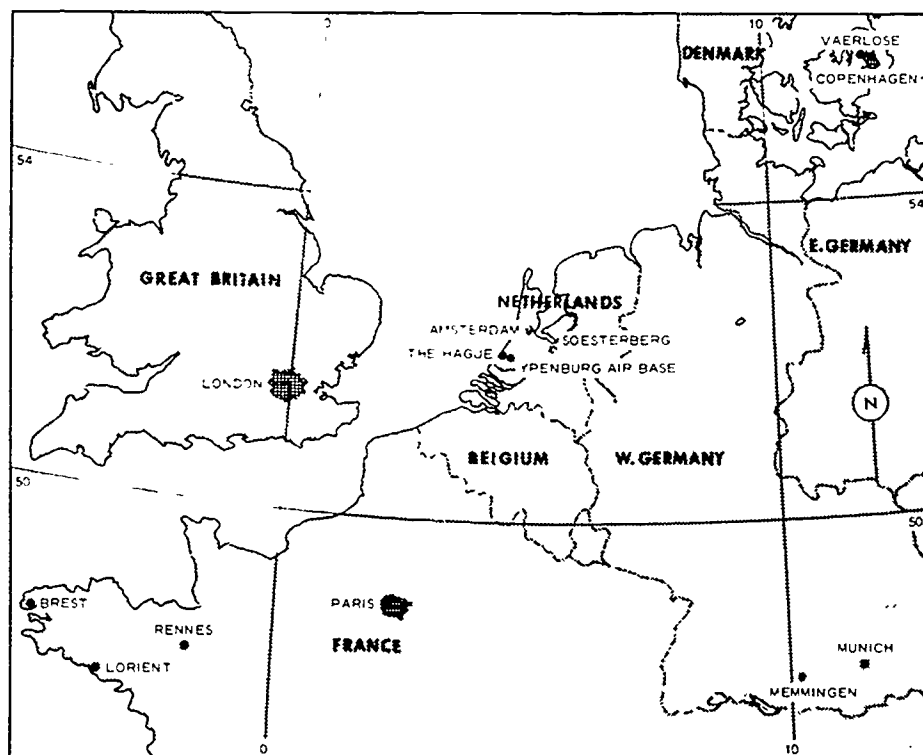


Fig. 3-1. Map of Netherlands OPAQUE Station location.

infrared turbulence, atmospheric turbidity, standard meteorological quantities, and aerosol particle size distribution. Of these data, the visible extinction, infrared transmittance, and meteorological data were particularly appropriate for this study. The atmospheric turbidity measurements were not included in this analysis because in the fog, when the infrared signals became most significant, the pyrheliometer data were offscale. The aerosol particle data would be of particular interest too, however the instrument was not yet installed during the periods analyzed here. Aerosol data were recorded in later seasons, however they were not available to us at the time of this analysis.

Thus, after some preliminary study of all the parameters, the analysis effort was directed primarily to those parameters summarized in Table 3.1.

The last column in Table 3.1 lists the number of available data points per measurement period. Each hourly measurement period lasted 4 minutes.

3.2 Instrument Discussion--Visible

Two measurements of visible extinction were available, the data from the Eltro transmissometer (1000m path length) converted to extinction coefficients, and the scattering coefficient from the AEG point visibility meter. The goal of the program was to achieve a measurement accuracy of $\pm 20\%$ in scattering coefficient and $\pm 2\%$ transmittance. For the purposes of this analysis, these numbers will be used as the most probable measurement accuracy. (See Appendix B.) The $\pm 2\%$ transmittance corresponds to an uncertainty in extinction coefficient of about 5% midrange, increasing to 30% or more near the limits of the reported transmittances. In practice it is found that the transmissometer indicates somewhat clearer air than the nephelometer does at the high transmittance end of the scale. Otherwise, the offsets between the

instruments are not particularly systematic. On some days, the two instruments are in agreement within close tolerance all day. On other days there is a significant nearly constant offset, while on others there is a variable offset.

In view of these uncertainties in the visible extinction, we initially chose for infrared comparison two sets of 5 days in which the two visible instruments were consistently in reasonably close agreement. The outlines of the prediction scheme were developed based on this 10 day sample. The analysis was then extended to three 3-month seasons. In the 9 month sample analysis, the comparisons with infrared extinction were made using both the nephelometer data and the transmissometer data. The nephelometer data have yielded slightly more consistent results. Because of this consistency, the final results in this report have been based on calculations using the nephelometer data.

3.3 Instrument Discussion--Infrared

The Barnes infrared transmissometer operates over a 500 meter path, and is intended to achieve a $\pm 2\%$ measurement accuracy. It was recognized quite early in the OPAQUE program that there were difficulties with the standard calibration procedure [Shand (1978)]. As a consequence, a different calibration scheme was evolved [Shettle and Fenn (1978) and Kohnle (1979)]. Basically, the data are searched for a clear day with low aerosol and water vapor content, i.e. a day with meteorological range ≥ 20 km, relative humidity $\leq 80\%$, dewpoint temperature $\leq 10^\circ\text{C}$, and no precipitation. (These criteria could not always be met.) On such a day, the aerosol extinction should be a minor portion of the total extinction, and the LOWTRAN calculation of total extinction should have optimal accuracy (Shettle, 1980). Thus a calibration constant can be determined by comparing the measured transmittance on this clear day with the transmittance

Table 3.1. Measured Variables Used for Analysis

	Symbol	Variable	Instrument*	Wave band	Units	Data Points
Visible	S	Scattering coefficient	Nephelometer (AEG Point Visibility Meter)	photopic	km^{-1}	4
	SF	Extinction coefficient	Transmissometer (Eltro)	photopic	km^{-1}	4
Infrared	T1 T5	Transmittance (3-5)	Transmissometer (Barnes)	3.4-5.0 μm	-	2
	T2	Transmittance (8-12)		8-12 μm		1
	T3	Transmittance (13-13)		8.25-13.2 μm		1
Meteor	T _{air}	Temperature	Thermometer	-	$^\circ\text{C}$	1
	RH	Relative humidity	Hygrometer	-	%	1
	RR	Rain rate during meas	Rain rate meter	-	mm/hr	1
	RF	Rain fall past hour	Precipitation meter	-	mm/hr	1
	WS	Wind speed at 10m and 2m	Wind speed meter	-	m/sec	1
	WD	Wind direction at 10m and 2m	Wind direction meter	-		1

*reference Van Schie (1976)

predicted by LOWTRAN (including the aerosol portion). The uncertainty in the calibration constant (determined on a clear day) results in an uncertainty in the calibration aerosol extinction from other days which becomes quite small in haze, mist, or fog. This uncertainty is discussed quantitatively in Section 5.2.

4. DATA REDUCTION

4.1 Derivation of Aerosol Extinction Coefficients

It is convenient to convert the visible and infrared data to aerosol extinction coefficients. This conversion expedites both the evaluation of the variations in the measured data and the comparison to models.

The visible data were supplied in the form of total extinction coefficients. The reported extinction coefficients range from .1 to about 30 km⁻¹, while the molecular or Rayleigh component is about .01 km⁻¹. Since this Rayleigh component is much less than the instrumental uncertainty, the measured data were treated as aerosol extinction coefficients. Within each 4-minute measurement period, a beginning, ending maximum, and minimum value were given. All four measurements were used in the analysis, but the results presented here are for the average of the beginning and ending points.

The infrared data were supplied in the form of total transmittance over a 500m path. In some cases, the calibration correction mentioned in Section 3 had already been applied. In other cases the correction factor was supplied and the data were corrected accordingly. The aerosol transmittance was then computed using the following equation.

$$T_{aer} = T_{meas} / [T_{H_2O}(t, t_d) \cdot T_{Mol}(t)] \quad (4-1)$$

In this computation, the water vapor (water molecule) and molecular (air molecule) transmittances (T_{H_2O} and T_{Mol}) were computed using the following equations from Shettle (1978a).

$$T_{H_2O}(t, t_d) = 1 - (c_1 + c_2 \cdot t) \exp[(d_1 + d_2 \cdot t) t_d] \quad (4-2)$$

$$T_{Mol}(t) = e + f \cdot t \quad (4-3)$$

These equations, derived by Shettle on a partly empirical and partly theoretical basis, represent average broadband transmittance, derived from the transmittances of Lowtran, as in Eq (2-2). The appropriate filter responses of the instrument were used in Shettle's derivation. The accuracy of Eqs. (4-2) and (4-3) relative to LOWTRAN is better than 1%. The constants of the equations for the Netherlands instrument [from Shettle (1978a)] are given in Table 4.1.

Since Eq (4-2) includes dewpoint temperature as an input, it was necessary to convert the reported relative

Table 4.1. Constants for Molecular and Water Vapor Transmittance Computation - Netherlands.

	Computation Constants		
	3.4-5.0 μm	8-12 μm	8.25-13.2 μm
c_1	$6.536 \cdot 10^{-2}$	$5.553 \cdot 10^{-2}$	$4.929 \cdot 10^{-2}$
c_2	$-2.658 \cdot 10^{-4}$	$-2.796 \cdot 10^{-4}$	$-3.011 \cdot 10^{-4}$
d_1	$4.751 \cdot 10^{-2}$	$6.661 \cdot 10^{-2}$	$7.538 \cdot 10^{-2}$
d_2	$-3.913 \cdot 10^{-4}$	$2.044 \cdot 10^{-3}$	$-2.370 \cdot 10^{-5}$
e	$8.661 \cdot 10^{-1}$	$9.919 \cdot 10^{-1}$	$9.949 \cdot 10^{-1}$
f	$1.40 \cdot 10^{-4}$	$3.8 \cdot 10^{-5}$	$1.8 \cdot 10^{-5}$

humidities to dewpoint temperatures. This was done using the following equation from Shettle (1978b).

$$t_d = \frac{(19.772 \cdot t) + [\ln(RH/100) \cdot (269.9 + t)]}{19.772 - \ln(RH/100)} \quad (4-4)$$

Thus the results of Eq. (4-4) are used as input to Eq. (4-2). Equation (4-2) is used along with Eq. (4-3) as input to Eq. (4-1), using the measured temperatures and relative humidities. Equation (4-1) yields the aerosol transmittance, which is then converted to aerosol extinction using the following equation

$$\alpha_{aer} (\text{km}^{-1}) = \frac{-\ln T_{aer}}{r} = \frac{-\ln T_{aer}}{.5 (\text{km})} \quad (4-5)$$

Thus the aerosol extinction is derived from the measured total transmittance and the computed molecular and water vapor transmittance at the time of measurement. Since the aerosol extinction is reasonably spectrally invariant within these bands, this extinction will not be significantly range dependent.

For the 3-5 μm band, a beginning and ending measurement were supplied for each 4-minute period. Both were used in the analysis, but most of the plots utilize the beginning measurement.

Another quantity used for comparison to the aerosol extinction was the seasonal median of water vapor and molecular extinction effective over a 500m path. For this quantity, the molecular and water vapor transmittances over 500m were computed using Eqs. (4-2) and (4-3) (which derive from LOWTRAN). These transmittances were then converted to effective 500m extinctions using Eq. (2-5), since the application here is transmitted radiance. These extinctions showed little variation within each season, so the median molecular and water vapor extinction was used in various figures and tables. These median 500m effective extinctions were not used in the computation of aerosol extinction, they were used only for general comparison to the aerosol extinction.

5. DATA ANALYSIS--DEVELOPMENT OF THE BIN CONCEPT

5.1 General Parameter Relationships

The general relationships between the infrared aerosol extinction and the other parameters may be conveniently illustrated using scatter plots. The plots in Sections 5.1 through 5.4 illustrate the data from one season: June, July and August 1977. Similar plots have been generated for two additional seasons, but are not included in the report. They look nearly identical to the plots from Summer '77, and the general comments in this section apply equally to all three seasons.

For this analysis, the data during rain are deleted. Rain data are expected to be characterized by less difference between infrared extinction and visible extinction. Since the scattering properties are expected to be significantly different for rain, it was decided to omit the rain cases. The following data points were omitted: any data points which indicated rain during the measurement period or rain during that hour; and any points for which either rain measurement was not recorded, which were thus indeterminate.

Figure 5-1(a&b) shows scatter plots of the IR aerosol extinction coefficient (α_{aer}) vs the visual aerosol extinction coefficient (S), in the 3-5 and 8-12 μm regions. The median effective molecular and water vapor extinction (labeled α_{Mol+H_2O}) is included for comparison. In Fig. 5-1 there is a fair amount of statistical scatter, but in general the IR extinction increases as the visual does (for this analysis, since we are dealing exclusively with the aerosol extinction in the IR bands, it is convenient to refer to it

simply as extinction). The squared correlation coefficient, r^2 , between $\log \alpha_{aer}$ and $\log S$ (with $\alpha_{aer} \leq .01$ omitted) is 26% at 3-5 μm and 21% at 8-12 μm . Thus the relationship is not tight enough for S alone to be an accurate predictor, yet there is definitely some information in the value of S . Much of the variation in Fig. 5-1 is expected because of instrumental uncertainty. This will be discussed later in this section.

Figure 5-2(a&b) shows aerosol extinction (α_{aer}) at 3-5 μm vs relative humidity (RH) and aerosol extinction (α_{aer}) at 8-12 μm vs RH . The IR data in Fig. 5-2 have a systematic and reasonable behavior with respect to the relative humidity. Over most of the relative humidity range, the IR extinctions are low, i.e. mostly between 01 and .1 km^{-1} , and there is little apparent variation with relative humidity. Above humidities of about 94% there are a large number of high infrared extinctions between 1 and 10 km^{-1} or higher. High infrared extinctions are expected to occur in the presence of large droplets which should normally be associated with nearly saturated air.

It is interesting to note in these figures that the highest infrared extinctions were associated with measured relative humidities near 95%. These data points often occurred during periods when the measured RH values were constant for several hours. The constant values vary from one day to the next, and are typically values such as 94.8% and 95.3%. The constant RH signal and the high values of IR extinction lead us to believe that the hygrometer was saturated, and that the true relative humidities were probably close to 100%. The expected instrumental uncertainty is about 5% for the hygrometer. (See humidity correction in Appendix B)

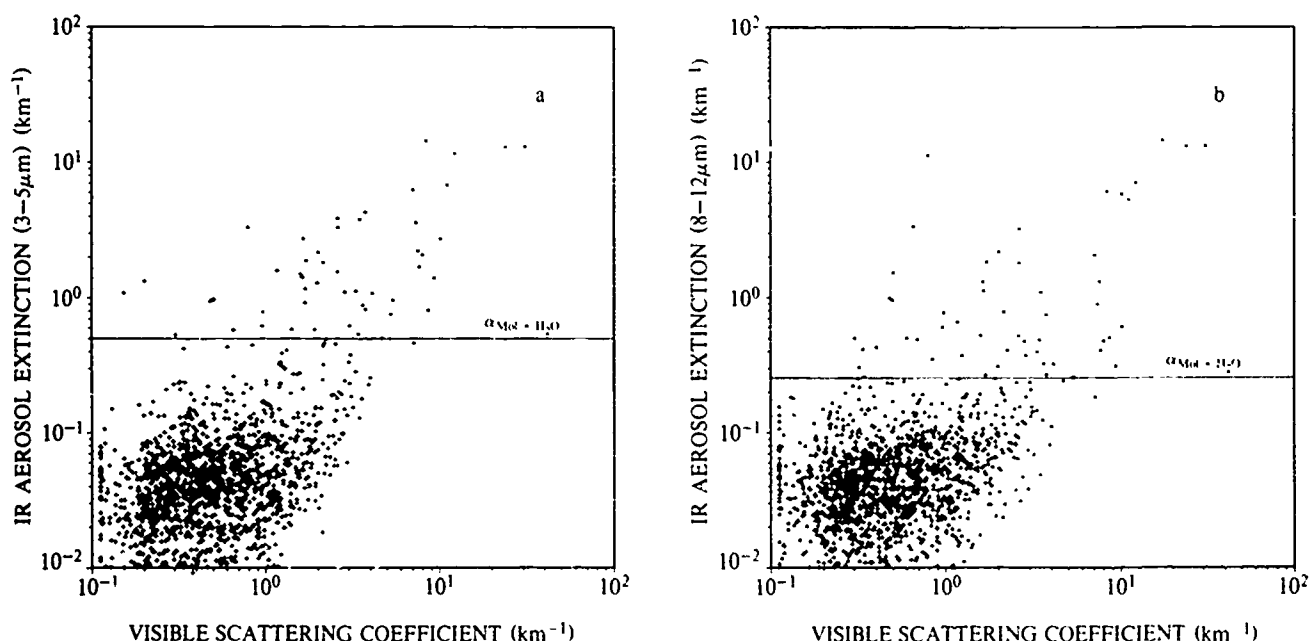


Fig. 5-1. Infrared aerosol extinction vs visible scattering coefficient

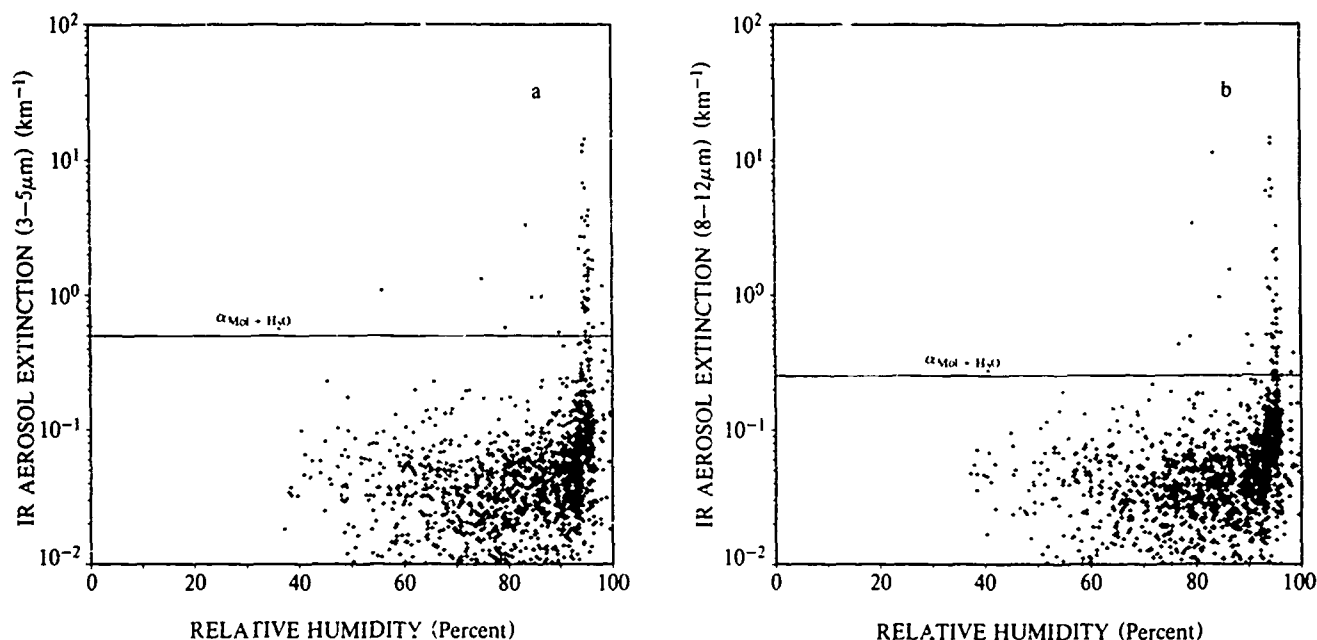


Fig. 5-2. Infrared aerosol extinction vs relative humidity.

The early 10-day studies yielded no systematic relation between infrared aerosol extinction coefficient and absolute humidity. Consequently this plot was not generated for the 3-month intervals. This result is corroborated by Bakker (1981) who reported an analysis of a 3-month Fall 1978 sample of Netherlands data. He notes "A possible interpretation of our results is that for relative humidities ≥ 0.90 it is the amount of liquid water [rather than water vapor or absolute humidity], present in the form of drops in rain or aerosols in fog that determines the infrared transmission of the atmosphere".

Figure 5-3 illustrates the scatter plot for the visible extinction coefficient (S) vs the relative humidity. The high visible extinctions, like the high IR extinctions, occur only at high relative humidities. An analysis of these high extinctions reveals that even when both the measured visual extinction and relative humidity are quite high (suggesting the presence of fog and large droplets), the measured infrared extinction is high for only a small portion of the cases.

Thus, both S and RH have predictive value. That is, the infrared aerosol extinctions tend to increase with the visual extinction S . The highest infrared aerosol extinctions are found at high relative humidities, but even when both S and RH are high, the infrared extinction is not always high. Thus, the goal is to devise the best scheme which makes use of the information in both parameters. Before this scheme can be presented, it is important to evaluate how much of the observed variation in the parameter relationships might be attributed to uncertainty in the aerosol extinction.

5.2 Infrared Aerosol Extinction Uncertainties

In evaluating the variation in the infrared aerosol extinction, there are four main sources of uncertainty to consider. These are the measurement uncertainty, the uncertainty due to the non-simultaneity of the data, the

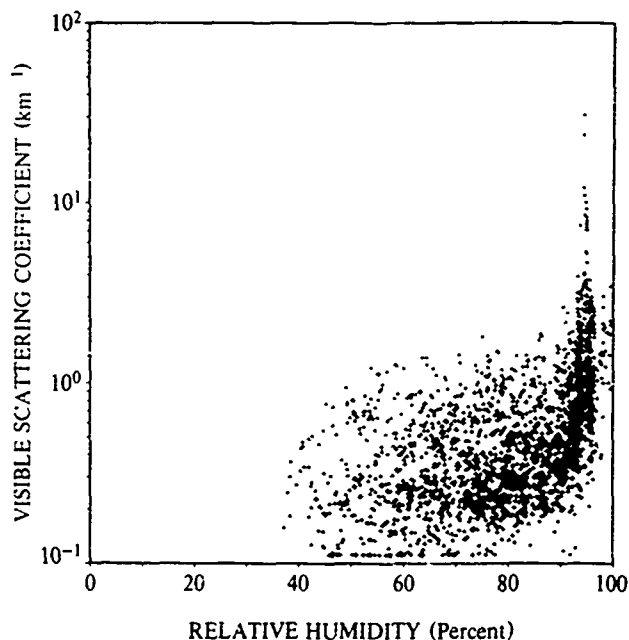


Fig. 5-3. Visible scattering coefficient (S) vs relative humidity (RH), summer 1977

uncertainty associated with the calibration procedure, and the uncertainty resulting from the molecular extinction. These four issues will be discussed in the following paragraphs. (See Appendix C)

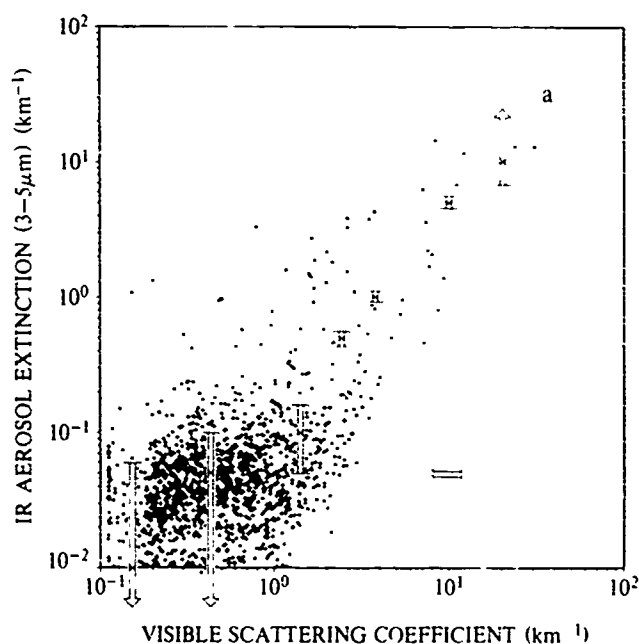
The projected level of accuracy for the infrared measurements was about $\pm 2\%$ in total transmittance. This corresponds to a variable uncertainty in aerosol extinction, as shown in Table 5.1.

Table 5.1. Aerosol Extinction Uncertainty for $\pm 2\%$ Uncertainty in Total Transmittance.

Aerosol Extinction α_{aer}	Aerosol Extinctions Resulting from 2% Change in Total Transmittance			
	3-5 μm		8-12 μm	
	$\alpha_{aer}(T + .02)$	$\alpha_{aer}(T - .02)$	$\alpha_{aer}(T + .02)$	$\alpha_{aer}(T - .02)$
.01	.04	.06	.04	.06
.05	.00	.10	.00	.10
.1	.05	.15	.05	.15
.5	.43	.57	.44	.56
1	.92	1.09	.93	1.08
5	4.46	5.75	4.51	5.65
10	6.86	∞	7.05	∞

The values in Table 5.1 were computed using the equation (see Appendix C)

$$\alpha_{aer} = \frac{-\ln\left(e^{-5(\alpha_{aer} + \alpha_{Mol+H_2O})} \pm .02\right)}{.5} - \alpha_{Mol+H_2O} \quad (5-1)$$



because it is $\pm 2\%$ of total transmittance. For this computation the median molecular plus water vapor extinction for Summer '77 was used, i.e. $.50 \text{ km}^{-1}$ at $3-5\mu m$ and $.25 \text{ km}^{-1}$ at $8-12\mu m$. Note that the uncertainty corresponding to $\pm 2\%$ total transmittance is primarily a function of the magnitude of the aerosol extinction, as may be seen in Table 5.1. The uncertainty depends only slightly on the magnitude of the molecular and water vapor extinction, (or on the relative contribution of aerosol to total extinction) resulting in slightly different values in Table 5.1 for the $3-5\mu m$ band and the $8-12\mu m$ band. Figure 5-4(a&b) shows these error bars superimposed on the plots of α_{aer} vs S (from Fig. 5-1). These figures also show the projected $\pm 20\%$ uncertainty in visible scattering coefficient, which is constant in S . (See Appendix B.)

In Fig. 5-4, note that most of the variation at the clear end, i.e. for S less than about 1 km^{-1} , can be explained simply by the projected infrared measurement uncertainty. For conditions where S is greater than about 1 km^{-1} , the variation in the infrared extinction becomes greater than the projected measurement uncertainty. Thus in this upper region, for $S > 1 \text{ km}^{-1}$, there is a significant amount of variation which might be explained by some predictor such as S or RH .

Although the plot includes only infrared aerosol extinctions α_{aer} greater than $.01 \text{ km}^{-1}$, the data set includes a significant number of points which are closer to 0 or negative, as would be expected from the error bars illustrated in Fig. 5-4. Using analysis of variance, in which the range in S was divided into about 10 bins, the variance in α_{aer} within each of these bins was computed. For this

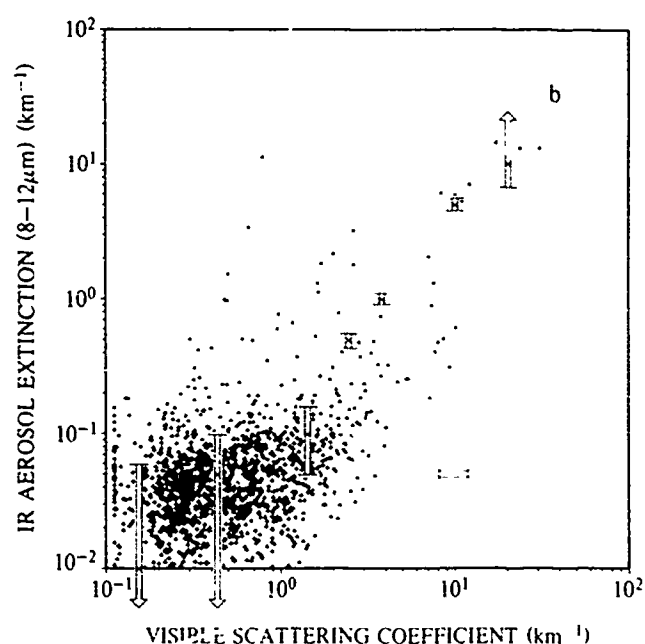


Fig. 5-4. Uncertainty in infrared aerosol extinction associated with a 2% uncertainty in measured IR transmittance (vertical bars). Horizontal bar represents a $\pm 20\%$ uncertainty in visible scattering coefficient.

analysis, all the non-rain data were used, including the negative points. The variance in each bin was then compared with the projected uncertainty at the midpoint for each bin.

The measured variation was found to be less than or equal to the projected measurement uncertainty for all the bins with S less than about 1. Here the variations in the measurements of α_{aer} are dominated by measurement uncertainty, and should not be predictable from other considerations. When S becomes greater than 1 km^{-1} , however, the observed variation is much more than the measurement uncertainty, and it should be possible to explain or predict some of the variation in α_{aer} .

The second source of uncertainty mentioned earlier is the uncertainty due to the non-simultaneity of the data. At the Netherlands station, each hour's data taking occurred during a four minute period. Since the IR and visible data are not simultaneous, this could contribute to the scatter observed in Figs. 5-1 and 5-2. Figure 5-5 compares the measurements of $3\text{-}5\mu\text{m}$ aerosol extinction which were taken at the beginning and end of each four minute period. Comparing Fig. 5-5 (final α_{aer} vs beginning α_{aer}) with Fig. 5-1(a) (beginning α_{aer} vs S) shows that the variation in infrared extinction during the four minutes is much less than the observed variation in infrared extinction at any given value of S . The squared correlation constants, r^2 are 26% for Fig. 5-1(a) and 74% for Fig. 5-5.

Thus while Fig. 5-4 illustrates that for S greater than about 1 km^{-1} , there is more variation than can be explained by measurement uncertainty, Fig. 5-5 illustrates

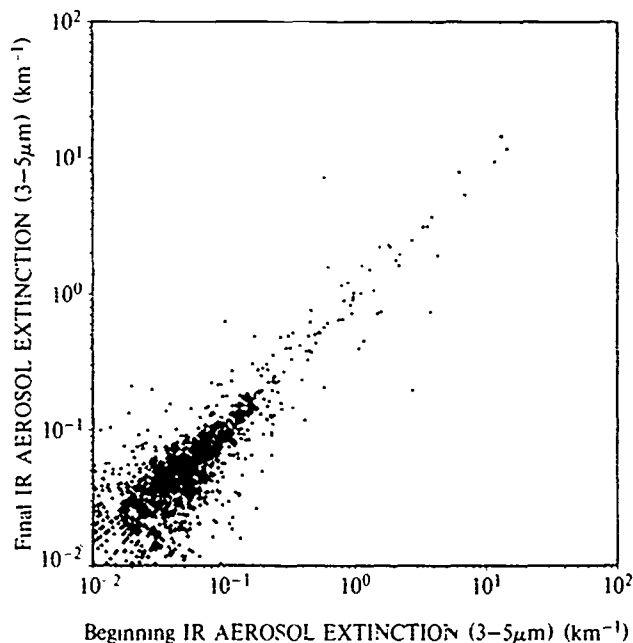


Fig. 5-5. Final vs beginning infra-red aerosol extinction coefficient at $3\text{-}5\mu\text{m}$ for each 4 minute measurement period

that this variation is not due primarily to the non-simultaneity of the data.

The variations in S during the four minute period were also studied by comparing the maximum with the minimum S and the beginning with the final S . These variations are quite small relative to the variation in Fig. 5-1.

The third source of uncertainty is the calibration correction scheme mentioned in Section 3.3. All of the reported data have been corrected by a calibration constant determined during data periods with high visibility and low water vapor content. During such periods, the aerosol extinction should be low so the LOWTRAN estimated extinction should be quite accurate. The calibration constant is determined by comparing the measured value with the LOWTRAN value during the calibration periods.

If there were no IR extinction measurement noise during the calibration periods, this technique would force the mean IR extinction to match LOWTRAN whenever it is clear. In actual practice, there is measurement noise during the calibration periods, so that there will be an uncertainty in the calibration constant. Also, there will be some uncertainty in the calibration constant due to uncertainty in the visual extinction, temperature, and dewpoint used to compute the LOWTRAN extinction during the calibration period. Both of these uncertainties are minimized by averaging as many points as possible to determine the calibration constant. In general it is safe to say that when the measured extinctions are high, they will not be significantly affected by the calibration correction, but as conditions approach the conditions of the calibration period, the average aerosol extinctions will be increasingly affected by the calibration correction.

The fourth source of uncertainty results from the subtraction of the molecular and water vapor extinctions from the total extinction to yield the aerosol extinction. The molecular and water vapor extinctions are functions of the temperature and the relative humidity. An uncertainty of 1° in temperature results in an uncertainty of $.007 \text{ km}^{-1}$ and $.014 \text{ km}^{-1}$ in the final infrared aerosol extinctions at $3\text{-}5\mu\text{m}$ and $8\text{-}12\mu\text{m}$ respectively. An uncertainty of 10% in relative humidity yields an uncertainty of $.018 \text{ km}^{-1}$ and $.03 \text{ km}^{-1}$ in the final extinction at $3\text{-}5\mu\text{m}$ and $8\text{-}12\mu\text{m}$ respectively. These uncertainties will have only a small effect on the low extinctions and will not significantly affect the high extinctions.

The net effect of the various sources of uncertainty should be as follows. When the visual extinction is low, i.e. $S < 1 \text{ km}^{-1}$, the infrared aerosol extinction is generally low (as shown in Fig. 5-1). In this regime the measurement uncertainty should yield large standard deviations. The use of the calibration constant should force the average infrared aerosol extinction to be close to LOWTRAN; how close the average is will depend on the number of measurements averaged to determine the calibration constant. At higher values of infrared extinction, these uncertainties should have little effect, but there should still be a finite but small uncertainty due to the non-simultaneity of the data. The effects of the temperature

and relative humidity uncertainties on the infrared extinctions should be small relative to these effects.

In summary, the error analysis showed that when the infrared extinction was low, most of the variation could be attributed to measurement uncertainty. When the infrared extinction was high, the variation could not be attributed to measurement uncertainty. It is therefore reasonable to try to relate the variations in the high infrared extinctions to predictor variations.

5.3 Method to Sort Infrared Extinctions

Taking into consideration the conclusions resulting from the scatter plots, summarized in Section 5.1, and the results of the error analysis, summarized in Section 5.2, the goal is to devise the most reasonable means of estimating infrared aerosol extinction.

For these data, the aerosol extinction is usually much less than the median molecular and extinctions. (In Figs. 5-1 and 5-2 the median molecular plus water vapor extinction is given. The molecular and water vapor extinction varies with temperature and humidity, however within each season its standard deviation was low.) Conveniently, the regime which is dominated by measurement uncertainty is the region of low infrared aerosol extinctions, in which the uncertainty in aerosol extinction represents a small uncertainty in the total extinction. That is, when the aerosol extinction is low the variations are not meaningful due to measurement uncertainty and they are not significant relative to the molecular and water vapor extinctions. However, when the aerosol extinction is high the variations are both meaningful (relative to measurement uncertainty) and significant (relative to the molecular and water vapor extinctions).

In view of these considerations, it was most important to try to develop some mechanism for sorting out the incidence of high infrared extinctions (or the incidence of high infrared to visible extinction ratios). If the low infrared extinctions could be isolated by some criteria in a lower bin, they could be treated with a stochastic model. The remaining data would go into an upper bin. The upper bin would hopefully include all of the high infrared extinctions. These extinctions would be high enough that their variations become more significant relative to the instrumental noise, and they would also be high enough relative to the molecular and water vapor extinctions that it would be more important to study their variations.

The really high infrared aerosol extinctions are expected to occur when near condensation conditions result in suspended water droplets of size about equal to the wavelength or larger. This condition is defined as mist or fog depending on whether the visibility is greater than 1 km, or less than or equal to 1 km [McIntosh (1963) and Proulx (1971)]. In particular, McIntosh defines mist as: "A state of atmospheric obscurity produced by suspended microscopic water droplets or wet hygroscopic particles. The term is used for synoptic purposes when there is such obscurity and the associated visibility exceeds one km: the corresponding relative humidity is greater than about 95

percent. The particles contained in mist have diameters mainly of the order of a few tens of microns." Thus a reasonable approach is to define an upper bin which should include all of the mist and fog incidents.

It should be noted that in the U.S., the term mist is popularly used to describe drizzle, we are using the term not to mean drizzle, but as defined above. Also it should be noted that it is common field practice to report this mist condition as thin fog, judging by the comments of local weather offices and sample weather reports from the U.S. and Europe [see Table 6-1 of Duntley *et al.* (1973) and Table 6-3 of Johnson *et al.* (1979a)].

Thus in order to isolate the high infrared extinctions in an upper bin, a reasonable approach is to attempt to isolate those conditions with large suspended droplets, i.e. mist and fog. For this data base, it was most effective to use two predictors to define the upper bin and the lower bin. First, the visible extinction is required to be greater than 1 km^{-1} (visibility ($\equiv 3 S$) $< 3 \text{ km}$) for the data to be included in the upper bin (mist and fog bin). The $S > 1 \text{ km}^{-1}$ cutoff was chosen because it is a reasonable threshold for mist, this is where the instrumental noise becomes less significant, and this is the threshold above which high IR aerosol extinctions begin to occur. The additional requirement for the high bin data is that RH must be greater than or equal to about 94%. (The cutoff used was $\log(1-RH/100) = -1.2$, or $RH = 93.7\%$). This threshold limits the bin to near condensation cases. The choice of 94% as opposed to 95% is required due to the uncertainty in the hygrometer. This cutoff allows inclusion of the very high infrared extinctions observed at relative humidities above 94% (Fig. 5-2). Those points not included in the upper bin, i.e. those with $S \leq 1 \text{ km}^{-1}$ or $RH < 94\%$, are included in the lower bin. (See Appendix B.)

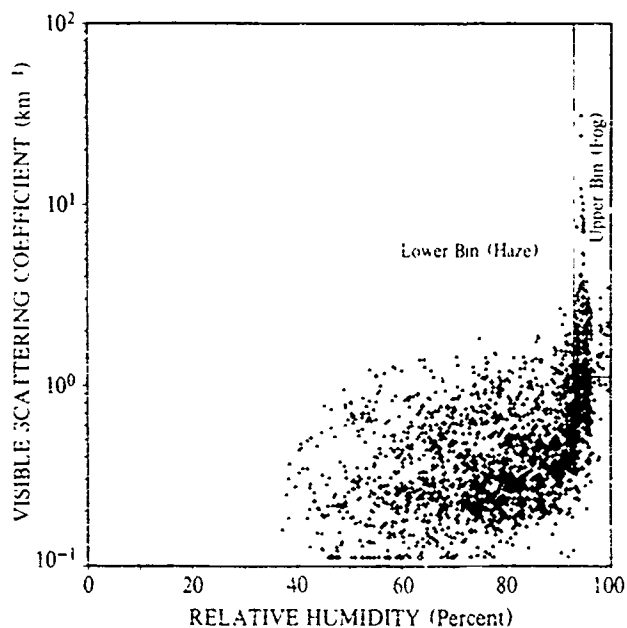


Fig. 5-6. Visible extinction and relative humidity thresholds for definition of the upper bin (Mist) and the lower bin (Haze)

Figure 5-6 illustrates the separation of data into the lower bin, consisting primarily of clear to haze conditions, and upper bin, consisting primarily of mist and fog. Theoretically, one would expect this sorting mechanism to separate the bulk of the low infrared extinctions from the high infrared extinctions. In the next section we will show how well the sorting scheme worked

5.4 Results of Sorting the Data

The results of sorting the data are shown in Fig.

5-7(a&b) for the 3-5 μm waveband, and Fig. 5-7(c&d) for the 8-12 μm waveband. These figures are histograms of α_{aer} . They show the number of occurrences for each .05 km^{-1} interval in α_{aer} . Figure 5-7(a&c) shows the aerosol extinctions from the upper bin, defined by $S > 1 \text{ km}^{-1}$ and $\log(1-RH/100) \leq -1.2$. The remaining aerosol extinctions are included in the lower bin, shown in Fig. 5-7(b&d), and defined by $S \leq 1 \text{ km}^{-1}$ or $\log(1-RH/100) > -1.2$. The negative values shown on these plots are the result of the measurement uncertainties discussed in Section 5.2.

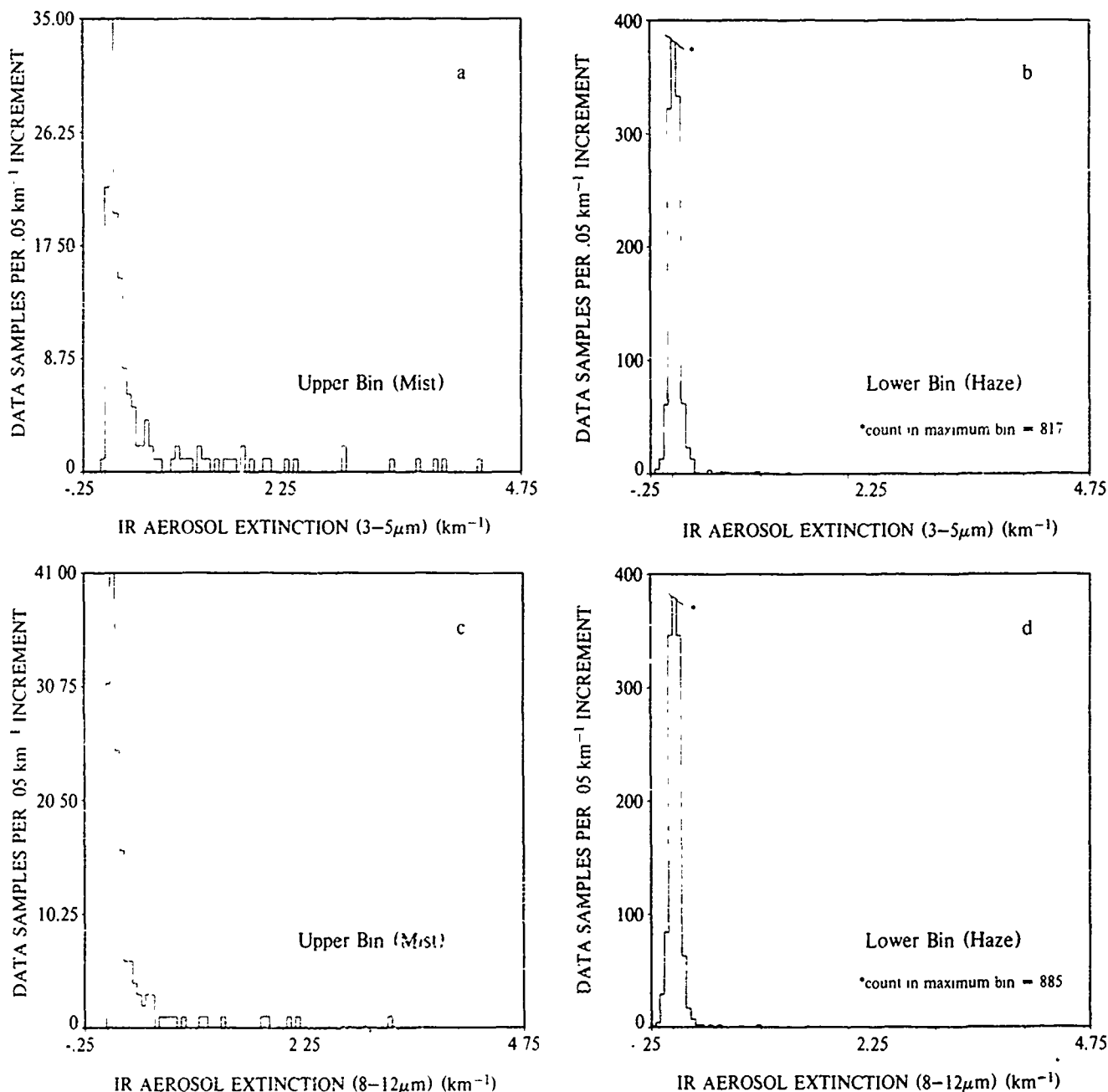


Fig. 5-7. Histograms of infrared aerosol extinction, 3-5 μm upper bin (Mist), 3-5 μm lower bin (Haze), 8-12 μm upper bin, and 8-12 μm lower bin.

From these plots, one can see that the method was reasonably successful in sorting out the high infrared extinctions. Nearly all the high infrared extinctions are included in the upper bin. The bins do not appear to be improved by slightly changing the thresholds. If the cutoffs were raised in either parameter, (i.e. if one used a higher S or higher RH cutoff), then too many high infrared extinctions were included in the lower bin; if the cutoffs were lowered in either parameter, then more low extinctions were included in the upper bin. Also, we found the use of both parameters as predictors necessary. If either parameter were used alone, then a large number of low extinctions were thrown into the upper bin.

Note that the upper bin, while including most of the high extinctions, also includes a great many low extinctions. As shown in later sections, the resulting large variation in α_{aer} in the upper bin is not due to instrumental uncertainty, but appears to be the result of variations in the aerosol properties.

5.5 Application of the Sorting Mechanism to Other Seasons

Although it is reasonable to expect that most of the high IR extinctions would be associated with mist and fog episodes, it is important to explore the effectiveness of the S and RH cutoff criteria with an extended data base. Two other 3-month seasons were chosen. June, July and August of 1978; and December 1977, January 1978, and February 1978. We designated the three 3-month seasons Summer '77, Summer '78, and Winter '77.

The scatter plots of the other two seasons looked very much like the scatter plots from Summer '77 illustrated in Section 5.1. The sorting mechanism described in previous sections were applied to the other two seasons, and worked very well. In each season, the lower bin includes very few occurrences of high infrared extinction. The data for all three seasons have been converted to cumulative frequency plots, as shown in Fig 5-8(a-f). These cumulative frequency plots show, for each value of α_{aer} , the percentage of cases with infrared aerosol extinction less than or equal to that value. (Note the scale change at $\alpha_{aer} = .3$.) In all cases, the low extinctions are much more prevalent in the lower bin, and the high extinctions are essentially isolated in the upper bin.

The median values of infrared aerosol extinction and the standard deviations for each bin are summarized in Tables 5.2 and 5.3. The median values correspond to the 50% values in Fig. 5-8. In these tables the seasonal changes are much less than the differences between the upper and lower bins. In all cases the seasonal changes are well within the standard deviations of the bins. These standard deviations are strongly influenced by a few high values, however they give a general idea of the variability. In the lower bin, both the median values and the standard deviations are in all cases very low relative to the median molecular and water vapor extinctions.

For the upper bin, the median values are in all cases (i.e. all seasons and filters) much higher than the medians

Table 5.2. Bin Statistics, Infrared Aerosol Extinction (α_{aer} at 3-5 μm)

Season	Upper Bin (Mist) Aerosol Extinction		Lower Bin (Haze) Aerosol Extinction		Molecular + H_2O Extinction	
	Median	STD	Median	STD	Median	STD
Summer '77	15	2.23	025	12	50	03
Summer '78	085	42	019	047	49	02
Winter '77	16	2.75	012	077	43	02

Table 5.3. Bin Statistics, Infrared Aerosol Extinction (α_{aer} at 8-12 μm)

Season	Upper Bin (Mist) Aerosol Extinction		Lower Bin (Haze) Aerosol Extinction		Molecular + H_2O Extinction	
	Median	STD	Median	STD	Median	STD
Summer '77	11	2.02	025	12	26	04
Summer '78	087	28	024	048	25	04
Winter '77	072	2.37	007	078	14	03

for the lower bin. More significantly, the standard deviations are quite large in the upper bin, even relative to the magnitude of the molecular extinction. Thus in the upper bin the variations become more significant, and worth looking at in greater detail.

Thus by using two predictors for sorting, the visible extinction and the relative humidity, one can create two bins: a bin which consists almost entirely of low values in infrared extinction, and a smaller high bin which includes nearly all the high values of infrared extinction as well as a significant number of low values. This sorting mechanism has been applied to two summer 3-month seasons and one winter 3-month season, and seems to apply well to all three seasons. This is a useful predictive scheme, in that it isolates the vast majority of the high extinctions in one bin.

6. DATA ANALYSIS--CHARACTERISTICS OF THE BINS

6.1 Characteristics of the Lower Bin

The lower bin or haze category is defined as the set of points with the visual extinction coefficients less than or equal to 1 (km^{-1}), or with $\log(1 - RH/100)$ greater than -1.2 (i.e. relative humidity < 94%). That is, the lower bin includes the lower end of the visual extinction and relative humidity ranges. This bin contains the vast majority of the points; 92% and 91% in the summers of '77 and '78, and 72% in the winter.

The infrared extinctions are consistently low in this bin. The observed variation is commensurate with a measurement uncertainty of $\pm 2\%$ transmittance as shown in Table 6.1. The observed variation in column 3 (STD in α_{aer}) is the standard deviation in the infrared aerosol

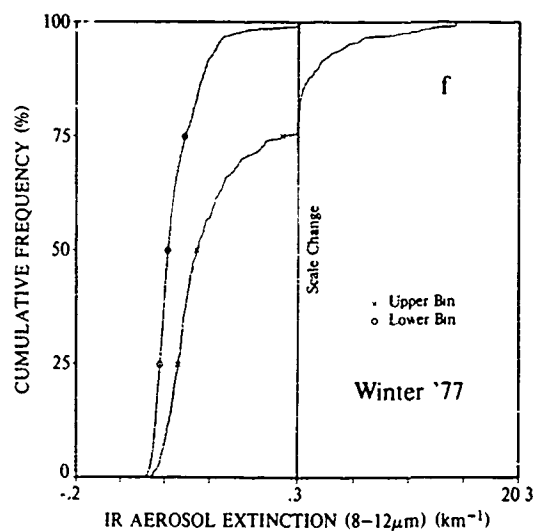
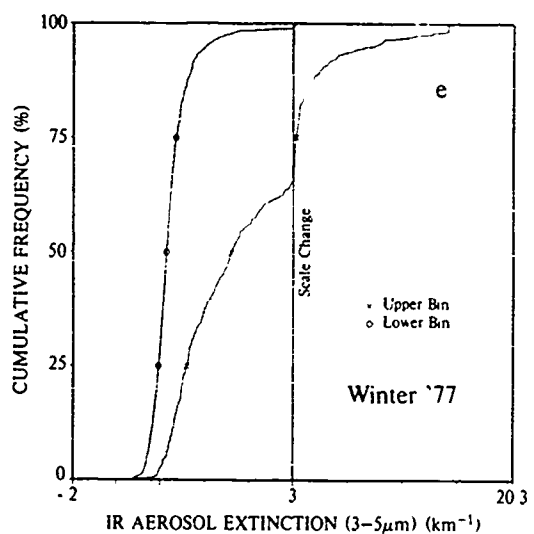
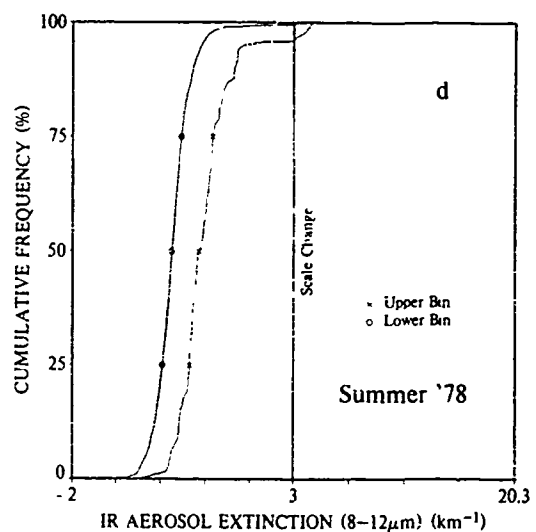
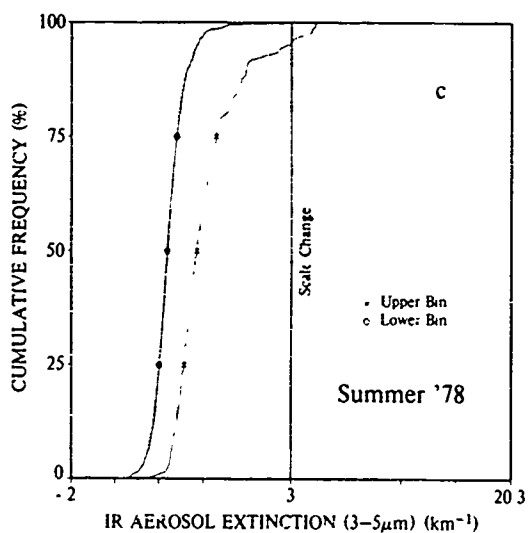
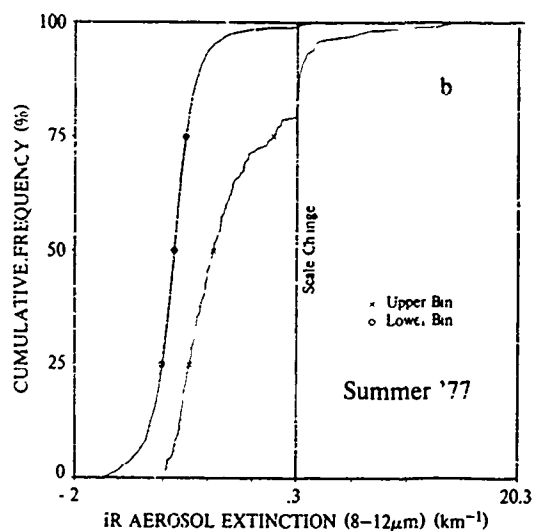
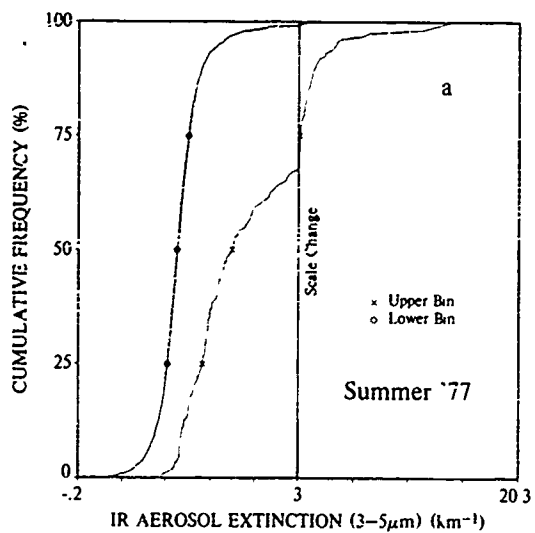


Fig. 5-8. Cumulative frequency for infrared aerosol extinction, one plot per season and filter, note scale change.

Table 6.1. Observed Variation in Infrared Aerosol Extinction (α_{aer}) for Lower Bin Compared with Projected Measurement Uncertainty ($\pm 2\%T$).

Filter	Season	STD in α_{aer}	Edited STD in α_{aer}	$\pm \alpha$ for 2%T at Medi α_{aer}
3-5 μm	Summer '77	12	08	05
	Summer '78	05	05	05
	Winter '77	08	06	05
8-12 μm	Summer '77	12	08	05
	Summer '78	05	05	05
	Winter '77	08	06	04

extinction α_{aer} in the lower bin. For two of the seasons, these standard deviations are strongly influenced by 1 or 2 very high values which may be spurious. Column 4 shows the standard deviations with these 1 or 2 exceptional points deleted. (For Summer '77, Summer '78, and Winter '77, the number of points deleted were respectively: 2 out of 1732, 0 out of 1240, and 1 out of 1112.) In column 5 the 2% uncertainty in transmittance has been converted to an uncertainty in α_{aer} at the median α_{aer} .

In Table 6.1, the observed variation in aerosol extinction in the lower bin is close to the projected measurement uncertainty. This means that whatever variation may have been caused by changes in particle size distribution or refractive index distribution of the aerosol, these variations are not much larger than the projected measurement uncertainty. One should not expect to be able to explain much of the real variation using other predictors because the real variations should be masked by measurement uncertainty.

Although systematic relations between the aerosol extinctions and available predictors were not expected (on the basis of the projected infrared measurement uncertainty), one can not be certain of the character and magnitude of the actual infrared measurement uncertainty. For this reason, some study was made of the parameter relationships in the lower bin. The ratio of infrared aerosol to visible extinction (α_{aer}/S) was evaluated and found to be more variable than the infrared aerosol extinctions. The character of the α_{aer}/S ratio changes appears to indicate that much of the ratio variation in the lower bin is due to measurement uncertainty in the visible extinctions at the clear end.

Also an attempt was made to further separate the lower bin cases into three bins on the basis of relative humidity and visible extinction. This method did not yield useful infrared aerosol extinction separations. This appears to support the expectation that the real variations in the lower bin are most probably masked by measurement uncertainty.

If further precision is desired in this lower bin it would be best to base the model on measurements taken with a longer path length instrument in the infrared as well as in the visible, to avoid much of the contamination caused by measurement uncertainty. For most purposes however, it is not necessary to resolve the variations in

the lower (haze) bin, since the aerosol extinctions are consistently low relative to the molecular and water vapor extinctions.

6.2 Estimation of Infrared Extinction for Haze Cases

This section describes how to use the statistics in the lower bin to provide an estimation of infrared aerosol extinction for at least this location. (The statistics may be site specific, however the general conclusions may apply more extensively.) As described in the previous section, it was found that the infrared aerosol extinction α_{aer} , rather than the extinction ratio α_{aer}/S , was better behaved in the lower bin. As can be seen in the histograms for the lower bin from Summer '77, in Fig. 5-7(b&d), the measured distribution of α_{aer} in the lower bin is not a normal distribution. Because of this, cumulative frequency tables such as Table 6.2 are used to describe the observed variance in infrared extinction. In Table 6.2 the two summers have been combined, to yield the most representative summer distribution.

This table may be interpreted as follows. The most typical value of measured infrared aerosol extinction for this location is given by the 50% value. The extinction that was exceeded only 5% of the time is given by the 95% value. Since much of this measured variation may be attributed to measurement uncertainty, one cannot say that the actual variation in the extinction is as large as implied in Table 6.2, however it is safe to say that the actual variation in the extinction is less than or equal to the measured variation. The negative values in Table 6.2 are an artifact of this measurement uncertainty.

Table 6.2 demonstrates what we have stated before, that in non-fog cases the aerosol extinction is consistently low. The 95% value is only about 1 km^{-1} . Even the 98% values are in most cases much lower than the molecular and water vapor extinction. As long as the visible extinction is less than 1 or the relative humidity is less than 94%, aerosol extinctions which approach molecular and water vapor extinction are very rare events.

The expected error in estimation for this location may be illustrated by comparing the measured values for one season with the values estimated on the basis of Table 6.2. The 50% values from Table 6.2 were used

Table 6.2. Cumulative Frequency, Aerosol Extinction (α_{aer}) Lower Bin (Haze)

Cum Freq (%)	Aerosol Extinction			
	Summer 3-5 μm	Winter 3-5 μm	Summer 8-12 μm	Winter 8-12 μm
98	15	16	14	18
95	100	100	099	118
90	076	068	078	071
80	053	042	056	062
50	022	012	024	0067
30	0058	0015	0054	0065
10	021	024	029	022
5	039	033	047	027
0	064	040	081	032

along with the measured α_{aer} values to compute the cumulative frequency for the square of the prediction error (the square of the difference between α_{aer} and the 50% value). The cumulative frequency for the error squared is shown in Fig. 6-1. In these plots, the x axis ranges from 0 to $(\alpha_{MOL} + \alpha_{H_2O})^2$ (rounded to a convenient number) using the median $\alpha_{MOL} + \alpha_{H_2O}$ from Summer '77. This scale was chosen because the absolute value of the error is of less importance than the magnitude of the error relative to the molecular and water vapor extinction. The median error² values are listed on the plot. These plots illustrate that the estimation errors are quite low. For both filters, the estimation errors are much less than the molecular extinction at least 99% of the time except for $\alpha_{aer}(8-12\mu m)$ in the winter, when the percentage drops to 97% due to the low molecular extinction.

It should be noted that the aerosol extinction shows very little spectral change within these wavebands (based on LOWTRAN5 and the LOWTRAN aerosol specifications). Thus the values in the cumulative frequency tables should apply reasonably well to most wavelengths within the two wavebands. To obtain total extinction, some technique such as the LOWTRAN model must be used to calculate the molecular and water vapor extinctions for the appropriate wavelength, since these are highly spectrally dependent. These derived model molecular and water vapor extinctions must be added to the estimated aerosol extinction to obtain the estimated total extinction coefficient.

6.3 Comparison of Measured and Model Haze Aerosol Extinctions

As an integral part of the program LOWTRAN5, the clear to haze aerosol extinction is calculated from Mie theory assuming several modelled particle size distribution and refractive index combinations, to represent rural conditions, urban, etc. Within each model, the relative size distribution and refractive index are allowed to vary with relative humidity, and the number density is normalized by the visual extinction. As a result, within each model, the infrared to visible ratio is a function only of relative humidity.

In another model by Huschke (1976), the 8-12 μm aerosol extinction is derived from a visible extinction and the ratio of infrared aerosol extinction to visible extinction. This ratio remains constant for relative humidities less than or equal to 50%, and the ratio increases to a ratio of 1.0 at a relative humidity of 100%.

Table 6.3 compares the measured low bin extinctions with the aerosol extinctions derived from the LOWTRAN5 and Huschke models. In this table, the measured Maximum, Median, and Minimum values are represented by the 98%, 50%, and 2% cumulative frequency measured extinctions. The model Maximum, Median, and Minimum values are the model values computed from the 98% cumulative frequency value of S and $RH=99\%$; from the median S and RH ; and from the minimum S and RH . The values in Table 6.3 are also plotted in Fig. 6-2.

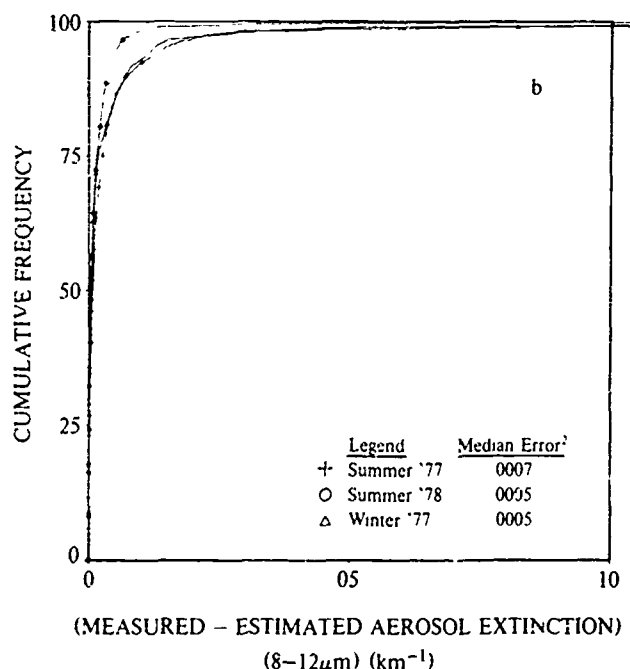
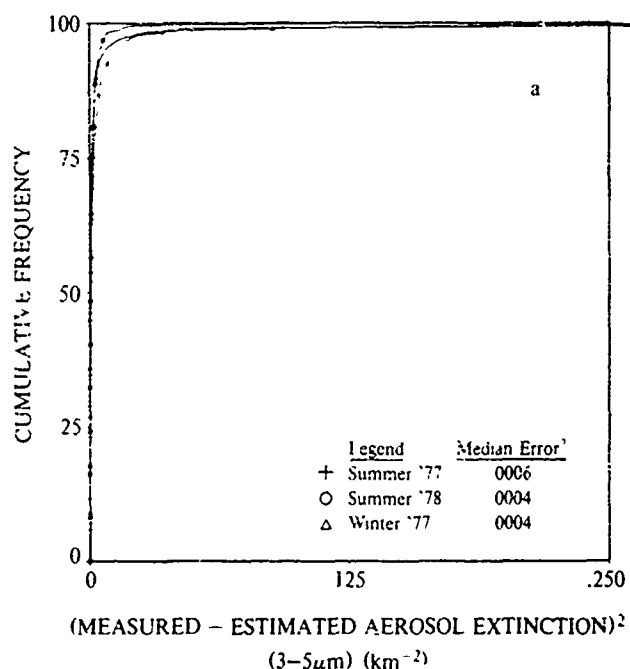


Fig. 6-1. Cumulative frequency of squared error of estimate for aerosol extinction at 3-5 μm , lower bin (Haze), three 3-month seasons

In Table 6.3 and Fig. 6-2, the median aerosol extinction is generally slightly lower than predicted by the LOWTRAN rural, urban, and maritime models, but slightly higher than predicted by the LOWTRAN tropospheric and Huschke models. The models all fall well within the range of measured extinctions.

6.4 Summary for Lower Bin (Haze) Cases

It was found that if either the visible extinction is less than or equal to 1 km^{-1} or the relative humidity is less than 94%, the data for this location may be classed in a low bin containing primarily clear to haze conditions. In this bin the infrared aerosol extinctions compare reasonably well to model predictions. The aerosol extinctions are consistently low relative to molecular and water vapor extinctions (thus they are a small portion of the total extinction) and may be represented by cumulative frequency of occurrence tables.

6.5 Characteristics of the Upper Bin

The upper bin was designed to include all the mist and fog data. It is defined as the set of points with the visual extinction coefficient S greater than 1 km^{-1} and $\log(1-RH/100)$ less than or equal to -1.2 (i.e. relative humidity $\geq 94\%$). That is, the upper bin includes the points which have both high visual extinction and high

Table 6.3. Comparison of Measured and Modelled Aerosol Extinctions for Lower Bin (Haze).

Season	Filter		Measured	LOWTRAN'S				Trop	Huschke
				Rural	Urban	Maritime			
Summer '77	3-5 μ m	Max	17	28	27	15	060	-	-
		Med	025	043	052	22	0061	-	-
		Min	-076	011	016	034	0013	-	-
	8-12 μ m	Max	17	18	16	71	028	85	-
		Med	-5	033	033	065	0065	012	-
		Min	-10	010	011	012	0018	0017	-
Summer '78	3-5 μ m	Max	11	23	22	12	049	-	-
		Med	019	026	033	13	0037	-	-
		Min	-044	011	015	033	0013	-	-
	8-12 μ m	Max	11	15	13	58	023	69	-
		Med	024	021	021	038	0040	0071	-
		Min	-048	010	011	011	0018	0016	-
Winter '77	3-5 μ m	Max	16	47	45	25	10	-	-
		Med	012	065	076	35	011	-	-
		Min	-040	011	015	034	0013	-	-
	8-12 μ m	Max	18	30	27	12	046	14	-
		Med	0067	047	047	11	0098	025	-
		Min	032	010	011	011	0018	0016	-

relative humidity. The bin contains about 8% of the points in the summer and about 22% of the points in the winter. It contains nearly all the high infrared aerosol extinctions, as well as a significant number of low infrared aerosol extinctions.

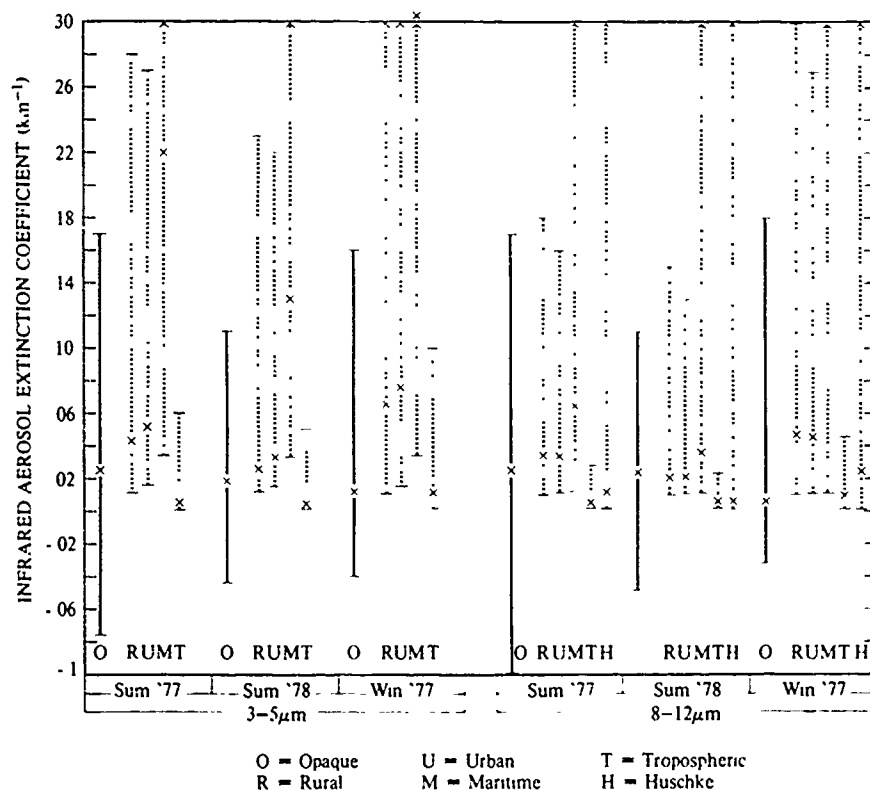


Fig. 6-2. Comparison of measured and model infrared aerosol extinctions, lower bin (Haze)

A test of the effectiveness of the bin thresholds may be performed by evaluating the ratio of infrared aerosol extinction to visible extinction, α_{aer}/S . This ratio is expected to approach values near 1 only in the presence of large droplets (of size $\sim 10\mu m$ or more) such as may occur in mist or fog. The histograms of α_{aer}/S for the upper bin from Summer '77, shown in Fig. 6-3, illustrate that there are a significant number of cases with ratios near 1 in this bin. By contrast, the lower bin has somewhat high ratios only when instrumental noise in S becomes large. In Fig. 6-3(a), there are several values with ratios above 1, however this is consistent with the $3-5\mu m$ LOWTRAN estimate for Radiation Fog Model 2 [Shettle and Fenn (1979)], which is 1.45.

An interesting feature of these histograms is the wide range in the magnitude of the α_{aer}/S ratio, and the prevalence of low ratios. The high ratios are distributed over the whole range in S , in the upper bin. Calculations utilizing the ending $3-5\mu m$ point (T5), and the beginning and ending visible points (SMAX and SMIN) showed similar distributions.

Like the α_{aer}/S ratio, the aerosol extinction α_{aer} varies over a wide range in the upper bin (ref. Fig. 5-8). The distribution in aerosol extinctions is summarized in Table 6.4. This table lists the percentage of cases which exceed three thresholds: $\alpha_{aer} > .1 \text{ km}^{-1}$, $\alpha_{aer} > \text{median } \alpha_{Mol+H_2O}$ for each season as listed in Tables 5.2 and 5.3, and $\alpha_{aer} > 1.0 \text{ km}^{-1}$.

Note that even in this mist bin, the infrared aerosol extinction is greater than the molecular and water extinc-

Table 6.4. Aerosol Extinction Values in Upper Bin.

Waveband	Season	% of Cases with α_{aer}		
		> 1	$> \text{Med } \alpha_{Mol + H_2O}$	> 1
$3-5\mu m$	Summer '77	63	24	17
	Summer '78	38	3	2
	Winter '77	62	28	17
$8-12\mu m$	Summer '77	54	23	8
	Summer '78	41	3	2
	Winter '77	43	34	13

tions only about 20% of the time, and greater than 1.0 km^{-1} only about 10% of the time, on the average. These high extinctions occur often enough to be important in many applications, however one certainly cannot assume that the infrared aerosol extinction will be high at all times.

Quite a bit of analysis has been done to determine whether the variations in infrared aerosol extinction in the upper bin could be related to some predictor. There is a tendency for the infrared aerosol extinction α_{aer} to increase along with the visible extinctions. As a result, the α_{aer}/S ratio is somewhat less variable than the extinction α_{aer} . There are a number of statistical tests which illustrate this, the most important being that the final error of estimate is reduced if the estimation is based on the median α_{aer}/S ratio rather than the median extinction α_{aer} .

Even though the ratio α_{aer}/S is better behaved than

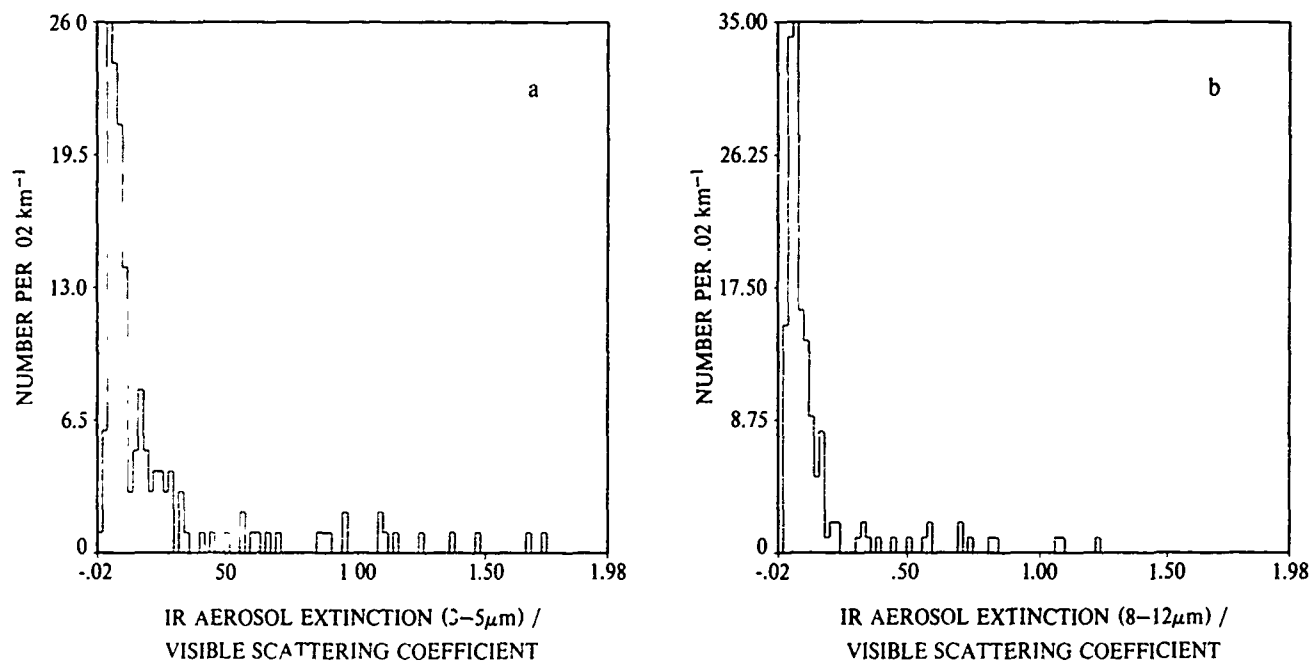


Fig. 6-3. Histograms of the ratio of infrared aerosol extinction to visible scattering coefficient, upper bin (Mist) summer 1977

the extinction α_{aer} , the ratio is quite variable (as noted earlier). By utilizing the ratio α_{aer}/S , we are essentially removing the effects of changes in the magnitude of particle number density. Changes in relative particle size distribution or refractive index would be expected to affect the α_{aer}/S ratio.

An analysis was made of the relationship between the α_{aer}/S ratio and a variety of parameters, such as wind speed and wind direction, and found no consistent relationships. Particularly the relationship between the α_{aer}/S ratio and the visible extinction S was studied, however analysis of variance showed that what little relationship existed between α_{aer}/S and S for the Summer '77 data was reversed in the Summer '78 data. Figure 6-4 shows α_{aer}/S vs S for Summer '77. Some sample error bars have been added to Fig. 6-4(a). The error in α_{aer}/S was computed assuming the errors in α_{aer} and in S are uncorrelated. The errors for Fig. 6-4(b) are of similar magnitude.

In Fig. 6-4, the high α_{aer}/S ratios are distributed over the whole range in S in the upper bin - they are not associated only with the highly turbid condition. The significance of this is that no matter what S threshold is used to define fog, there will still be a mixture of high and low ratios. Fog is internationally defined to have meteorological range ≤ 1 km, or $S \geq 3.9 \text{ km}^{-1}$. Looking at the cases with $S > 4 \text{ km}^{-1}$ in Fig. 6-4, one can see that at least half the points still have low ratios. Conversely, in the $1 < S < 4 \text{ km}^{-1}$ range, which is defined not to be fog, there are still a significant number of cases with high ratios. That is, in both mist and fog, the infrared to visible ratio is often high, but even in fog it is also often low.

Some of the variation in the infrared to visible ratio in the upper bin could potentially be related to relative humidity. We do not have a precise measure of relative humidity. The relative humidity measurement accuracy is about $\pm 6\%$, judging by the fact that there were a number of cases with constant relative humidity of about 94% associated with high infrared to visible ratios (which indicates the true relative humidity was most probably about 100%). Some of the data in the upper bin were almost undoubtedly saturated, but others may not have been, and we have no way to separate them. Future measurements using more precise instrumentation to determine relative humidity might allow one to partially separate the high ratios from the low ones.

It should also be noted that some of the variation in the α_{aer}/S ratio may be related to aerosol type. Some of these aerosols may have been advection fogs, and others may have been radiation fogs. The advection fogs are normally associated with large droplets and high infrared to visible ratios, while the radiation fogs are normally associated with small droplets and lower infrared to visible ratios. Examination of the synoptic and mesoscale meteorology would be useful in exploring this possibility.

6.6 Study of the IR Aerosol Extinction Persistence in the Upper Bin

In the previous section, it was found that even in the mist bin, the infrared aerosol extinction remained lower than the molecular and water vapor extinction about 80% of the time. The incidence of the high extinctions did not appear to be related to available predictors. It is

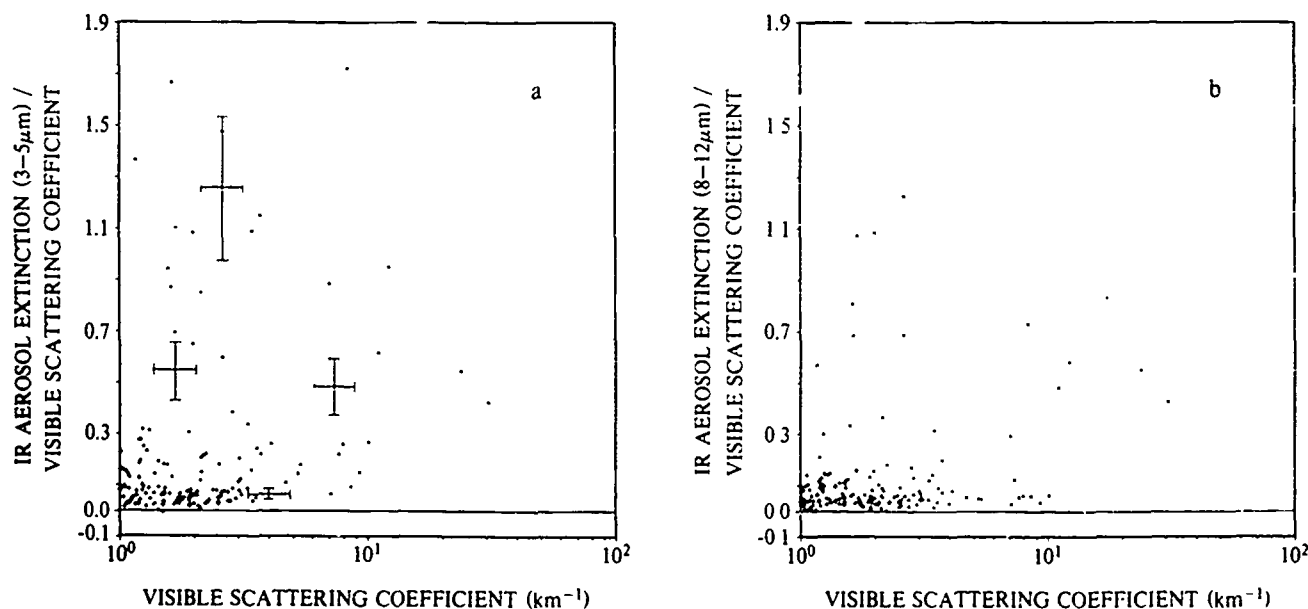


Fig. 6-4. Ratio of infrared aerosol extinction to visible extinction, α_{aer}/S , vs visible extinction $S (\text{km}^{-1})$, upper bin (Mist), summer 1977.

important to know how stable the infrared conditions were, i.e. how long the infrared aerosol extinctions persisted.

In the absence of significant periodic variations, the correlation coefficient between measurements of the same parameter at times 0 and t would be expected to decrease exponentially with time t according to the equation

$$r(t) = r(0)e^{-at} \quad (6-1)$$

where a is the relaxation constant, and $r(0)$ is the correlation coefficient for $\Delta\text{time}=0$. The value of $r(0)$ is related to measurement uncertainty. (See Appendix B.)

This type of calculation is called a persistence calculation. Note that these persistence calculations are not calculations of the correlation between the visible and infrared, nor are they frequency of occurrence calculations. Persistence calculations relate to the question of how stable a given parameter is with the passage of time. See Brooks and Carruthers (1953)

For this study, calculations were made of the time variations in the infrared as well as in the visible. Two correlations were run in the 3-5 μm waveband, one in the 8-12 μm waveband, and two in the visible. In the 3-5 μm band and the visible, the measurements taken at the beginning of each measurement period were correlated with those at the end of the 4-minute period, and were correlated with the values taken at the next measurement period 60 minutes later. The two resulting correlation coefficients may be represented by $r(4)$ and $r(60)$. For the 8-12 μm band, only $r(60)$ could be computed.

The squared correlation coefficients $r^2(4)$ and $r^2(60)$ are listed in Table 6.5. These statistics are based on $\ln \alpha$ or $\ln S$. The r^2 values for 60 minutes are fairly low in both the infrared bands, but somewhat higher in the visible band

The persistence correlations for the 3-5 μm waveband are plotted in Fig. 6-5. Note that the intercepts are slightly less than 1 as expected. The values of $r(0)$ for the 3-5 μm band are listed in column 2 of Table 6.6. (These values are approximate, due to the uncertainties in the extrapolation.) The $r(0)$ coefficients may be converted to estimates of standard errors using the following equation, which applies to normal distributions.

Table 6.5. Squared Persistence Correlation Coefficient (r^2), Upper Bin (Mist).

Season	r^2 (4 minutes)		r^2 (60 minutes)		
	Visible	3-5 μm	Visible	3-5 μm	8-12 μm
Summer '77	997	80	64	32	30
Summer '78	987	78	53	28	28
Winter '77	995	92	69	57	50

These squared correlation coefficients are based on the natural log (\ln) of the aerosol extinction coefficients

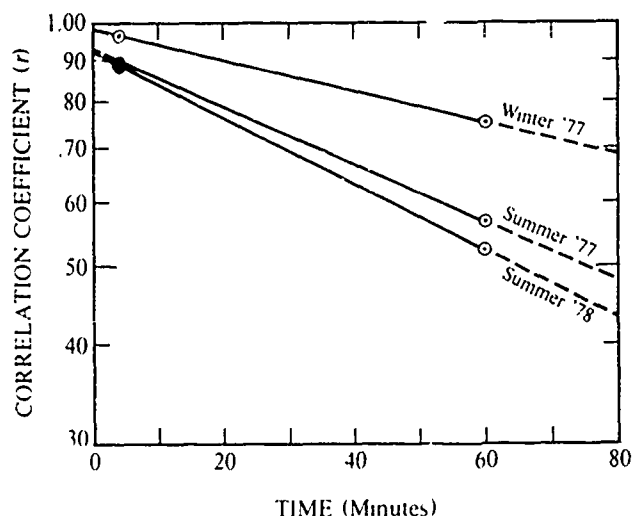


Fig. 6-5. Persistence correlation coefficient, r , for 3-5 μm , upper bin (Mist)

$$SE^2 = (1-r^2)\sigma^2 \quad (6-2)$$

where SE is the standard error and σ is the standard deviation in the predicted values. The resulting standard errors for time 0, listed in column 3 of Table 6.6, may be compared with a measurement uncertainty of $\pm 2\%$. This uncertainty corresponds to an uncertainty in $\ln \alpha_{\text{av}}(3-5\mu\text{m})$ (for the median value of $\alpha_{\text{av}}(3-5\mu\text{m})$ in the upper bin) of about 22-38%, which compares reasonably with the approximate standard error of 33-55%.

Column 4 of Table 6.6 lists the inverse of the relaxation constant, a^{-1} , (for 3-5 μm), converted to hours. This time is the interval over which the correlation coefficient would be expected to reduce to $1/e$, or .37. The time interval a^{-1} is short in the summer, lasting about 2 hours. Note that it is somewhat longer in the winter, indicating that the magnitude of infrared extinction at 3-5 μm was more persistent in the winter than in the summer

The inverse of the relaxation constant a^{-1} may also be calculated for the visible, since both $r(4)$ and $r(60)$ values were available. The resulting a^{-1} values, given in column 5 of Table 6.6, are significantly longer than the a^{-1} values for the 3-5 μm band. Thus the magnitude of the visible aerosol extinction apparently persists longer than the magnitude of 3-5 μm aerosol extinction for this fog bin. That is, the visible extinction is more stable than the infrared extinction. One conceivable cause for this might be that the large droplets are more transient than the small droplets

It is interesting to compute the 3-5 μm persistence correlation coefficient for the time duration of the average fog episode. The approximate duration of the average mist or fog period was calculated by determining the average number of consecutive hours during which the data fit into the upper bin. This average time interval is denoted t_4 in column 6 of Table 6.6. The expected correlation

Table 6.6. Related Persistence Statistics for Upper Bin (Mist).

	3-5 μm			Visible	Avg. Mist Interval t_A (hour)	2-5 μm
	Corr. Coeff. r (0 min)	Stan Err SE (0 min)	(Relax Const) $^{-1}$ a^{-1} (hour)	(Relax Const) $^{-1}$ a^{-1} (hour)		Corr Coeff for time t_A $r(t_A)$
Season						
Summer '77	.93	.55	2.1	4.3	3.8	.15
Summer '78	.92	.33	1.8	3.0	3.6	.12
Winter '77	.98	.38	3.9	5.1	5.6	.23

coefficient for this average time interval (based on Eq. 6.2) is listed in column 7 of Table 6.6. These correlation coefficients are very low, indicating that one cannot expect much persistence or stability in the infrared aerosol extinction during the average mist or fog period.

Thus these persistence calculations show that the infrared extinction is relatively unstable in the mist or fog. It varies on a faster time scale than does the visible. During the period of the average mist episode, there is sufficient variation in the IR extinction to result in a low self-correlation between the IR extinction values. These variations could quite possibly be due to short term variations in particle size distribution.

These persistence calculations bear particularly on the question of what is causing the large range in infrared to visible ratio. The important point is that the measurements do not show a steady IR to visible extinction ratio during a given episode, with different extinction ratios during other episodes on another day. (If that were the case one might suspect that the episode with the low ratios was not actually mist or fog.) What the measurements show is a series of episodes during which the visibility is

consistently reduced, and the relative humidity consistently high; and within each episode, the infrared extinction is varying over a large range, on a relatively short time scale.

It is perhaps helpful to give examples of mist episodes. Figure 6-6 shows two long but otherwise fairly typical mist episodes. Even though the relative humidity was over 94% and the visible extinction over 1 km^{-1} , both the IR aerosol extinction and the IR to visible extinction ratio are quite variable. Even during periods when the visible extinction was over 3 km^{-1} , the IR to visible ratio ranged from .2 to 1.2 during one episode and .2 to 1.0 during the other. These two are isolated examples of the IR variability within the mist episodes; the persistence statistics show quantitatively the extent to which this occurred generally.

In summary, the variations in infrared aerosol extinction appear to occur on a relatively short time scale. In the mist bin, the infrared aerosol extinction is high a significant portion of the time but less often than expected, and the extinctions do not persist over long periods.

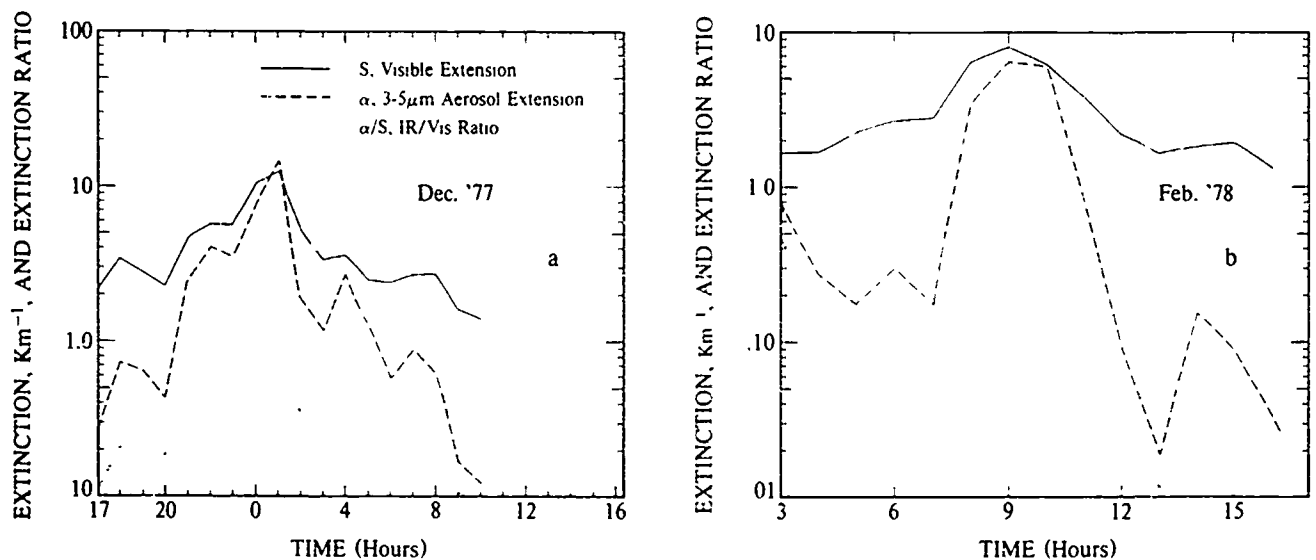


Fig. 6-6. Extinction variations within two mist episodes Dec. 15 at 1700 to Dec. 16 at 1000, 1977, and Feb. 1 from 0300 to 1600, 1978

A possible future approach to the problem of predicting the high infrared aerosol extinctions is discussed in Section 7. For the present, it appears that the ability to predict the extinction coefficient in the upper bin is probably limited by short term variations in infrared extinction, and that as a result one might profitably use a stochastic model for this bin. Although the character of the mist is such that one cannot give an exact value of infrared extinction for each value of a predictor, a stochastic model still yields useful accuracy, as will be shown in the next section.

6.7 Estimation of Infrared Extinction for Mist and Fog Cases

This section describes how to use the statistics in the upper (mist) bin to provide an estimation of infrared aerosol extinction for this location. As described in the previous section, it was found that for the upper bin (unlike the lower bin), the ratio α_{aer}/S was better behaved than the extinction α_{aer} . The distribution of the α_{aer}/S ratio is not a normal distribution, so as with the lower bin, it is necessary to use a plot or table of cumulative frequency of occurrence. The data from the two summers have been combined. Table 6.7 shows some cumulative frequency of occurrence values for each season and filter.

These tables would be used just as the tables for the lower bin. One would first use the visible extinction and relative humidity to determine that the upper bin is the appropriate bin to use. Then one would multiply the appropriate value of α_{aer}/S from Table 6.7 by the measured value of visual extinction to determine the estimated infrared extinction. (The appropriate value of α_{aer}/S to use would depend on the application; on whether one wanted the median value, for example, or perhaps the value that will not be exceeded 95% of the time.)

The expected error in estimation for this location is shown in Fig. 6-7. These values are based on the 50% value of α_{aer}/S . In Fig. 6-7(a&c), the range for the x-axis is the same as for Fig. 6-1, i.e. from 0 to the median Summer '77 value of $(\alpha_{MOL} + \alpha_{H_2O})^2$. The median error² values are listed on the figures. The errors are less than the molecular extinction about 80% to 95% of the time, depending on the season.

Table 6.7. Cumulative Frequency, Ratio of Infrared to Visible Aerosol Extinction (α_{aer}/S), Upper Bin (Mist)

Cum Freq (%)	α_{aer}/S			
	Summer 3-5 μm	Winter 3-5 μm	Summer 8-12 μm	Winter 8-12 μm
98	1.17	1.02	.70	.90
95	.87	.82	.42	.53
90	.31	.51	.16	.32
80	.16	.21	.099	.093
50	.060	.061	.053	.027
30	.040	.037	.037	.016
10	.024	.027	.020	.0021
5	.016	.0077	.012	.0060
2	.0085	.0025	.0046	.015

In the remaining 5-20% of the cases, the error can become quite significant, as illustrated in Fig. 6-7(b&d). These figures illustrate the same data as Fig. 6-7(a&c) plotted on a different scale.

As with the lower bin, the estimated aerosol extinction applies reasonably well to any wavelength within the measured wavebands. The estimate of total extinction would be obtained by using a model such as LOWTRAN to compute the molecular and water vapor extinctions at the desired wavelength, and adding these to estimated aerosol extinction.

6.8 Comparison of Measured and Model Mist and Fog Aerosol Extinctions

The measured data in the upper bin may be compared with the LOWTRAN5 model using the ratios of infrared to visible aerosol extinction α_{aer}/S . The measured ratios, listed in Table 6.8, may be compared with the ratios inherent in the aerosol portion of the model. The LOWTRAN5 ratios for the 99% relative humidity haze models and the fog models are listed in Table 6.9. Figure 6-8 illustrates the model to measurement comparison.

Comparing Tables 6.8 and 6.9, one can see that at least 50% of the measured ratios for each season fall lower than any of the model ratios except the tropospheric. In fact the 50% ratios for the high bin are lower than the rural, urban, or maritime ratios for any relative humidity. Thus many of the ratios are somewhat lower than predicted. The 80% cumulative frequency measured ratios from Table 6.8 compare well to the 99% RH values from Table 6.9. And the 95% or 98% cumulative frequency measured ratios compare well to the fog model ratios.

Table 6.8. Measured Ratios of Infrared to Visible Aerosol Extinction (α_{aer}/S), Upper Bin (Mist)

Cum Freq (%)	Summer α_{aer}/S		Winter α_{aer}/S	
	3-5 μm	8-12 μm	3-5 μm	8-12 μm
98	1.15	1.02	.70	.90
95	.87	.82	.42	.53
80	.16	.21	.099	.093
50	.060	.061	.053	.027
30	.040	.037	.037	.016

Table 6.9. LOWTRAN5 Ratios of Infrared to Visible Aerosol Extinction (α_{aer}/S), Fog and 99% Relative Humidity Haze Models

Model	Model α_{aer}/S	
	3-5 μm	8-12 μm
Rural 99%	.17	.11
Urban 99%	.17	.099
Mar 99%	.92	.43
Trop 99%	.037	.017
Rad Fog 1	1.22	.68
Rad Fog 2	1.45	.24
Adv Fog 1	1.08	1.23
Adv Fog 2	1.09	1.24

Thus in the upper bin, which is characterized by visual extinctions greater than 1 km^{-1} and relative humidities over 94%, some of the measured ratios are typically expected fog ratios, but many are typical haze ratios or lower.

One significant way in which these data differ from the LOWTRAN model is the manner in which these ratios in the upper bin vary. Based on LOWTRAN, one might expect to choose a model based on the recent air mass history or the current conditions. One would for example

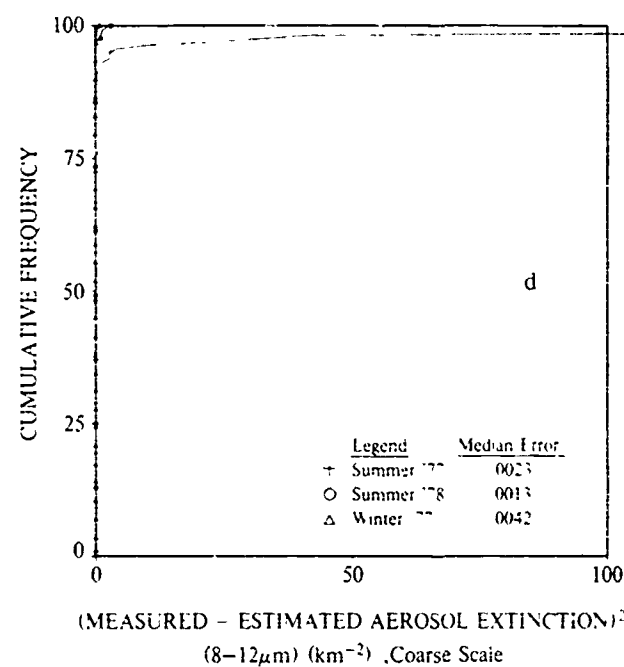
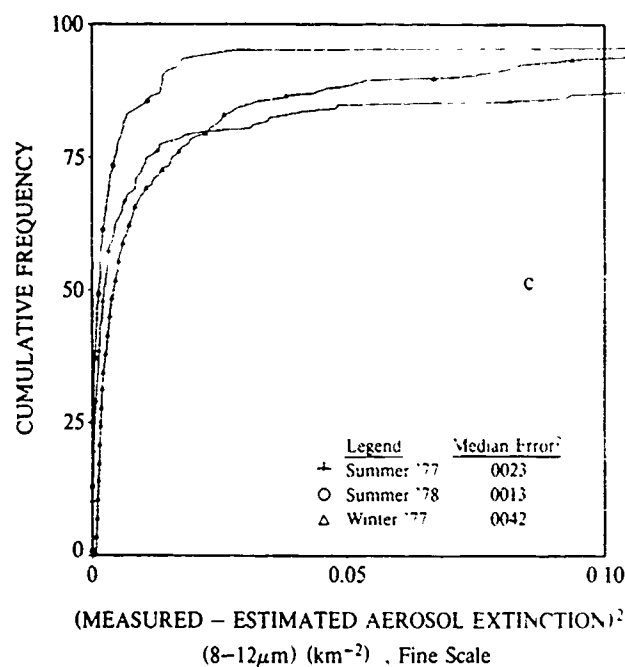
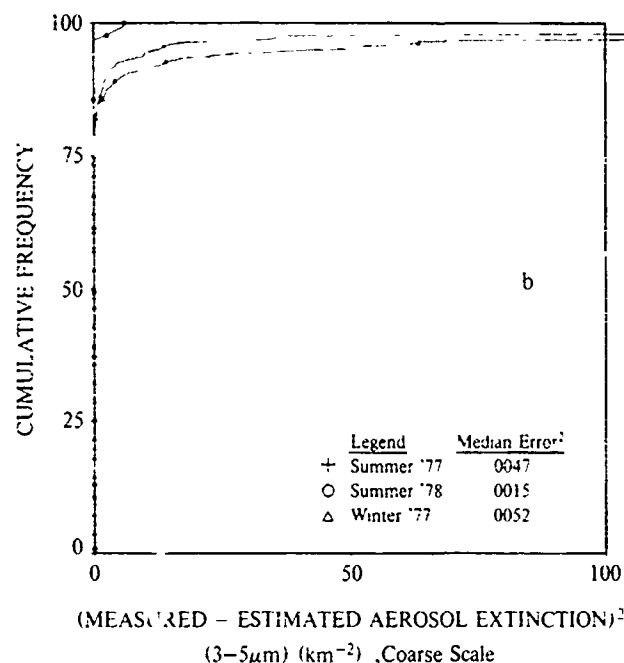
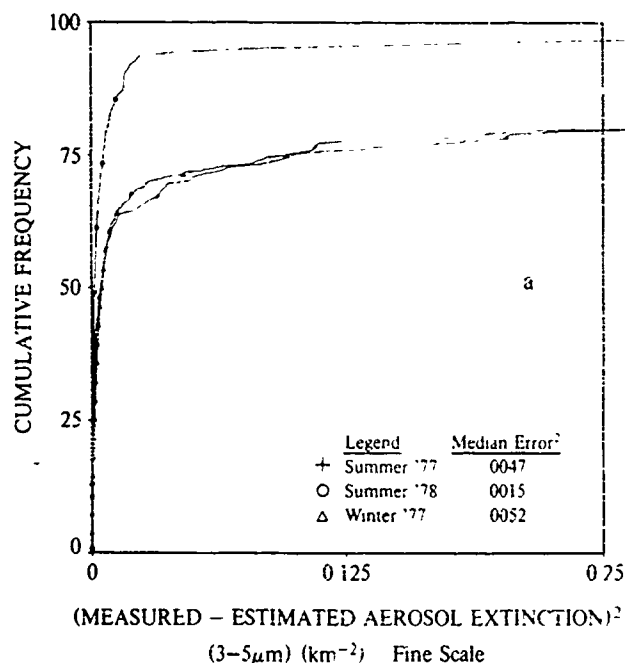


Fig. 6-7. Cumulative frequency of squared error of estimate for infrared aerosol extinction upper bin (Mist) three 3-month seasons per plot

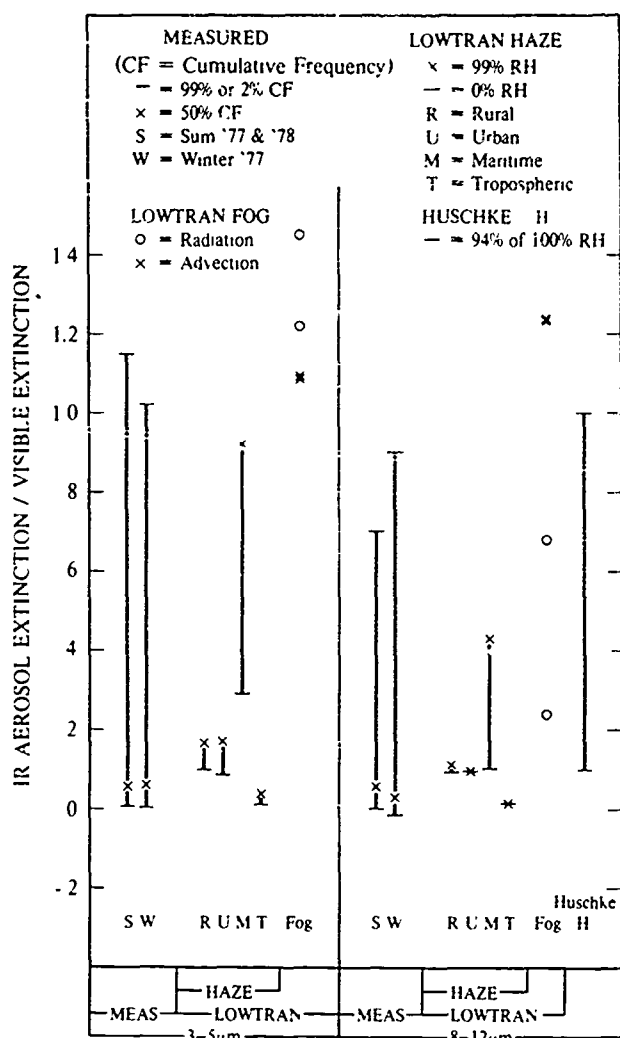


Fig. 6-8. Comparison of measured and model ratios of infrared aerosol extinction to visible extinction, upper bin (Mist and Fog)

choose the urban 99% model if fog had not formed, or one of the fog models if fog had formed. If this information is lacking, the LOWTRAN5 recommendation is to use 99% aerosol models for S of 2 to 4 km^{-1} , radiation fog for S of 4 to 10 km^{-1} , and advection fog for $S > 10 \text{ km}^{-1}$. From this model, one might expect the ratios to be reasonably constant for a fair time period. In fog, for example, one might expect to use ratios above 1 as long as the fog lasted. In contrast to this expectation, the OPAQUE data show that within a given episode of reduced visibility and high relative humidity, the infrared to visible ratio is quite variable, on a short time scale. Additionally, the high ratios are not distributed with visual extinction in the same way one might expect from the model. There are many high α_{aer}/S ratios in the $S \approx 1-2 \text{ km}^{-1}$ range, as well as low ratios at higher values of S . The variations in Table 6.8 do not appear to correspond to changes in conditions from non-fog to fog, but rather correspond to short term variations within the fog.

These results can explain one reason that experimentalists may obtain results significantly different from those predicted by LOWTRAN. Basically, LOWTRAN predicts one extinction for a given condition. These OPAQUE data show that the model extinction is a pretty good estimate of the median condition, but that the aerosol extinction varies significantly about that median as a result of short term variations in IR extinction, which may be associated with short term variations in particle size distribution.

The upper bin data may also be compared with the aerosol portion of the Huschke model. For the upper bin, the measured relative humidities are between 94% and 100%. This corresponds to a range of .1 to 1.0 in Huschke's 8-12 μm infrared to visible ratio. As may be seen in Table 6.8, some of the observed 8-12 μm ratios fall within this range, but most are lower. Again, the character of the variations is somewhat different from the Huschke model. Even in cases where the relative humidity is constant for a number of hours, and we believe the air to be saturated, i.e. at about 100% relative humidity, the infrared to visible ratio is quite variable due to the short term variations discussed earlier. This model, as well as the LOWTRAN model, might be improved by using a distribution of expected ratios rather than using one expected ratio.

6.9 Summary for Upper Bin (Mist) Cases

If the visible extinction is greater than 1 km^{-1} and the relative humidity is greater than or equal to 94%, the data for this location may be classed in an upper bin, or mist and fog bin. Even in this bin, the infrared aerosol extinction remains lower than the molecular and water vapor extinction (about .5 km^{-1} for 3-5 μm and .25 km^{-1} for 8-12 μm) about 80% of the time. The infrared aerosol extinctions exceed 1 km^{-1} about 10% of the time. The variations in infrared aerosol extinction occur on a relatively short time scale, so that the self correlation in the infrared extinction over the period of the average fog episode is quite low.

For this location, the infrared aerosol extinctions for the mist bin may be estimated reasonably well about 80% of the time through the use of cumulative frequency distributions of the infrared to visible aerosol extinction ratio. However, about 20% of the time this method will result in large estimation errors. It should be operationally important to develop mechanisms to predict or detect these 20% of the cases in which the aerosol extinction becomes large.

7. SUGGESTED FURTHER WORK TO ENHANCE THE ANALYSIS

7.1 Analysis of the OPAQUE Data

The results presented in this report are based on a large number of data samples--roughly 7000 hours worth of data--yet they represent just one station and three seasons (2 summer seasons and a winter season). A spot

check of a few other stations might yield further verification of the results of this study. It is reasonable to expect that the basic technique of dividing the data into two bins should be effective at other locations, however one would expect that the cumulative frequencies of the bins and the most effective bin thresholds are to some extent a function of season and location.

It would be particularly useful to look at the distribution of aerosol extinction in the upper bin and to determine the persistence of the aerosol extinctions in the upper bin for other locations. Perhaps the most important result of this study was finding that high infrared extinctions are less stable than expected in mist and fog. The OPAQUE data are ideal for determining the extent to which this is true at other stations. The Fall Netherlands data might be particularly interesting, since Janssen and van Schie (1981) note that high extinctions are much more frequent in the fall.

7.2 Further Experimental Work

One of the primary conclusions of this analysis is that high infrared extinctions occur less frequently than expected in fog, and have low persistence. The variations in infrared extinction appear to be the result of short term variations with time and space. As a result, if one is to predict the extinctions with greater accuracy than can be obtained with a stochastic model, one scheme worth considering is operationally feasible techniques to detect the presence of large droplets at the exact time and place the prediction is desired. Two parameters which may be strongly affected by the presence of large droplets are the wavelength dependence of aerosol scattering in the visible, and the shape of the phase function for directional scattering in the visible. Measurements which are affected by these parameters, such as measurements of the blue/red scattering ratio or measurements of forward/back scattering ratio might provide means of detecting those fog conditions which lead to high infrared aerosol extinctions. A feasibility experiment to determine the efficacy of these measurements might be well advised.

The above experiment might provide means of predicting the variations within the upper bin. If it becomes important to predict the variations in the lower bin, then it would be advisable to make additional measurements with much longer path length instruments both in the visible and the infrared. The lower bin suffers from the instrumental noise in both the visible and infrared, but longer path length transmissometers would measure this region more accurately. Since the lower bin extinctions are low relative to the molecular extinction, however, it should not be necessary to resolve this variation in the lower bin, for most operational purposes.

8. CONCLUSION

This report discusses an analysis of infrared and visible extinctions recorded in the Netherlands over three 3-month seasons. The data, recorded at hourly intervals during this period, were gathered as a part of the

OPAQUE program. They are preliminary releases data. (See Appendix B.)

It was found that the infrared aerosol extinctions could effectively be sorted into a clear to haze category and a mist to fog category. Two observations were required to determine the appropriate category: the visual extinction and the relative humidity. The use of either parameter alone yielded a much less effective categorization.

The haze category consisted of those points with visual extinction less than or equal to 1 km^{-1} or relative humidity less than 94%. (See Appendix B.) In this category the aerosol extinction coefficients were consistently low with respect to the water vapor and air molecule extinction. The median aerosol extinctions were about 0.1 to 0.2 km^{-1} . The extinctions may be represented by a cumulative frequency distribution of aerosol extinction, with a resulting error of estimate which is consistently low. The infrared aerosol extinctions in this non-fog category are reasonably close to model extinctions.

The mist to fog category consisted of those points with visual extinction greater than 1 km^{-1} and relative humidity greater than or equal to 94%. In this category, the aerosol extinctions are typically about 1 km^{-1} , with a significant number of cases between 1 and 10 km^{-1} or higher. Thus the mist bin includes the high values expected in fog, however these high values are surprisingly infrequent and transitory. The aerosol extinction is greater than the water vapor and air molecule extinction (about 0.5 km^{-1} at $3.5 \mu\text{m}$, about 0.25 km^{-1} at $8.12 \mu\text{m}$) in about 20% of the cases, and they persist for short periods relative to the visual extinction persistence and relative to the duration of the fog episodes.

When the aerosol extinctions in this mist category are high, they match the fog models reasonably well, but much of the time they are much lower. In contrast to the models, these data show the existence of high IR to visible extinction ratios at lower visual extinction thresholds, and show a great variability in infrared aerosol extinction within the fog.

The variance in infrared aerosol extinction within the fog was somewhat related to the variance in visual extinction. As a result, the infrared extinctions for the fog bin were best estimated through the use of the cumulative frequency distribution of infrared to visible aerosol extinction ratio α_{IR}/S .

Although the bin thresholds and resulting cumulative frequency distributions are applicable only to this location, the sorting scheme should be applicable to other locations as well. Perhaps the most important result of this work is the observation that even when both the visual extinction and relative humidity are high, indicating mist or fog, the infrared aerosol extinction remains quite variable on a short time scale, with high infrared aerosol extinction occurring frequently, yet less often than expected. Even if much higher thresholds for visual extinction were used to define the upper bin, the high infrared aerosol extinctions are still a minority.

As a result of this work, one may suggest two primary future avenues of investigation. First, interrogate the remaining OPAQUE data to determine the distribution and persistence of the infrared aerosol extinctions in the mist at other locations. Secondly, begin an experimental study to determine the feasibility of detecting large water droplet formation and thus the high infrared aerosol extinctions using measurements such as blue/red scattering ratios. The experimental approach would be to explore measurement techniques which are operationally feasible and which are theoretically expected to be effective in detecting large water droplet formation and thus high infrared aerosol extinctions.

9. REFERENCES

- Bakker, T. (1981), "Atmospheric Measurements in a Coastal Environment", AGARD Proceedings CP-300 Paper 9.
- Brooks, C. E. P., and N. Carruthers (1953), *Handbook of Statistical Methods in Meteorology*, Air Ministry, Meteorological Office, Her Majesty's Stationary Office, London.
- Duntley, S. Q. (1973), "Airborne Measurements of Optical Atmospheric Properties in Southern Illinois", University of California at San Diego, Scripps Institution of Oceanography, Visibility Laboratory, SIO Ref 73-24, AFGL-TR-73-0422.
- Fenn, R. W. (1978), "OPAQUE - A Measurement Program on Optical Atmospheric Properties in Europe, Vol. I. The NATO OPAQUE Program, Special Reports No. 211, AFGL-TR-78-0011.
- Fitch, B. W. and T. S. Cress (1981), "Measurements of Aerosol Size Distributions in the Lower Troposphere Over Northern Europe", University of California at San Diego, Scripps Institution of Oceanography, Visibility Laboratory, SIO Ref 81-18, AFGL-TR-80-0192.
- Huschke, R. E. (1976), "Atmospheric Visual and Infrared Transmission Deduced from Surface Weather Observations: Weather and Warplanes VI", Report R-2016-PR RAND, Santa Monica.
- Janssen, L. H. (1981), "A Comprehensive Survey of the OPAQUE Transmittance Measurements", Report PHL 1981-05.
- Janssen, L. H. and J. van Schie (1981), "Frequencies of Occurrence of Transmittances in Several Wavelength Regions during Three Years", *Appl. Opt.*, Vol. 21, No. 12, 2215-2223.
- Jennings, S. G., R. G. Pinnick, and H. J. Auvermann (1978), "Effects of Particulate Complex Refractive Index and Particle Size Distribution Variations on Atmospheric Extinction and Absorption for Visible Through Middle IR Wavelengths", *Appl. Opt.*, Vol. 17, No. 24, 3922-3929.
- Johnson, R. W., and J. I. Gordon (1979a), "Airborne Measurements of Atmospheric Volume Scattering Coefficients in Northern Europe, Winter 1978", University of California at San Diego, Scripps Institution of Oceanography, Visibility Laboratory, SIO Ref 79-25, AFGL-TR-79-0159.
- Johnson, R. W., W. S. Hering, J. I. Gordon, B. W. Fitch, and J. E. Shields (1979b), "Preliminary Analysis and Modelling Based upon Project OPAQUE Profile and Surface Data", University of California at San Diego, Scripps Institution of Oceanography, Visibility Laboratory, SIO Ref. 80-5, AFGL-TR-79-0285.
- Kneizys, F. X., E. P. Shettle, W. O. Gallery, J. H. Cherwynd, Jr., L. W. Abreu, J. E. A. Selby, R. W. Fenn, and R. A. McClatchey (1980), "Atmospheric Transmittance/Radiance Computer Code LOWTRAN5", AFGL-TR-80-0067.
- Köhne, A. (1979), "Barnes Calibration via LOWTRAN, some Aspects", *Forschungsinstitut für Optik, Tübingen*, OPAQUE AN-N/GE-7908.
- McIntosh, D. H. (1963), *Meteorological Glossary*, Meteorological Office, Her Majesty's Stationary Office, London.
- Nilsson, B. (1979), "Meteorological Influence on Aerosol Extinction in the 0.2-4.0 μm Wavelength Range", *Applied Optics*, Vol. 18, No. 20, 3457-3473.
- Pinnick, R. G., S. G. Jennings, P. Chýlek, and H. J. Auvermann (1979), "Verification of a Linear Relation Between IR Extinction Absorption and Liquid Water Content of Fogs", *American Meteorological Society*, Vol. 36, 1577-1586.
- Proulx, G. J. (1971), *Standard Dictionary of Meteorological Sciences*, Scientific and Technical Division, Department of the Secretary of State, Ottawa, Canada, McGill-Queen's University Press.
- Roberts, R. E. (1976), "Atmospheric Transmission Modeling Proposed Aerosol Methodology with Application to the Grafenwöhr Atmospheric Optics Data Base", *Proceedings of the Optical - Submillimeter Atmospheric Propagation Conference*, December 1976, DDR&E.
- Shand, W. A. Ed. (1978), "Barnes Intercomparison Trial-Pershore, September 1977", RSRE(C) Christchurch, Dorset, England, OPAQUE R7804.
- Shettle, E. P. (1978a), "Theoretical Transmittances for the OPAQUE Barnes Transmissometers", Air Force Geophysics Laboratory, Bedford, Mass., OPAQUE N/US-7805.
- Shettle, E. P. (1978b), "Analytic Expressions for the Atmospheric Water Vapor Content", Air Force Geophysics Laboratory, Bedford, Mass., OPAQUE N/US-7810.
- Shettle, E. P. (1980), "Procedure for Calibration of the OPAQUE IR Transmissometers via LOWTRAN Calculations", Air Force Geophysics Laboratory, Bedford, Mass., OPAQUE N/US-8001.
- Shettle, E. P. and R. W. Fenn (1978), "IR-Transmissometer Calibration, Comparison with LOWTRAN", Air Force Geophysics Laboratory, Bedford, Mass., OPAQUE N/US-7808.
- Shettle, E. P. and R. W. Fenn (1979), "Models for the Aerosols of the Lower Atmosphere and the Effects of Humidity Variations on Their Optical Properties", AFGL-TR-79-0214.

- van Schie, Jr. J. (1976), "Netherlands report to RSG.8 over the period May 1976 - October 1976", Physics Laboratory of the National Defense Research Organization TNO, OPAQUE D/NL-7608
- Whitby, K. T. (1978), "The Physical Characteristics of Sulfur Aerosols", *Atmos. Env.* Vol. 12, 135-159.
- Yue, G. K. and A. Deepak (1980), "Modeling of Growth, Evaporation and Sedimentation Effects of Transmission of Visible and IR Laser beams in Artificial Fogs", *Appl. Opt.* Vol. 19, No. 22, 3767-3774

10. ACKNOWLEDGEMENTS

Probably the most difficult and time-consuming part of any experimental study is involved in setting up the instruments, ensuring their accuracy, and recording the data. Consequently, I am indebted to Ir. T. Bakker, Ir. J. Van Schie and their associates of the Physics Laboratory of the NDRO-TNO, Netherlands for providing us with the data for this study.

Additionally, I would like to thank several individuals for their assistance during the preparation of this report and during the analysis which preceded it.

From the Visibility Laboratory, I would especially like to note the assistance of the following individuals. Mr. Wayne S. Hering, who suggested many of the analysis approaches such as the use persistence correlation, and made significant contributions to the data interpretation; Mr. Richard W. Johnson, for many invaluable discussions of the analysis; Mr. Nils R. Persson, for providing and/or helping train the author in the computer processing techniques; and Mrs. Alicia G. Hill, for careful and prompt word processing.

From the Air Force Geophysics Laboratory, Dr. Robert W. Fenn, Maj. John D. Mill, Mr. Eric P. Shettle, and previously Maj. Ted S. Cress provided valuable assistance and advice.

APPENDIX A

VISIBILITY LABORATORY CONTRACTS AND RELATED PUBLICATIONS

Previous Related Contracts:

F19628-73-C-0013, F19628-76-C-0004

PUBLICATIONS:

- Duntley, S. Q., R. W. Johnson, and J. I. Gordon (1972), "Airborne Measurements of Optical Atmospheric Properties in Southern Germany", University of California at San Diego, Scripps Institution of Oceanography, Visibility Laboratory, SIO Ref. 72-64, AFCRL-72-0255.
- Duntley, S. Q., R. W. Johnson, and J. I. Gordon (1972), "Airborne and Ground-Based Measurements of Opti-

cal Atmospheric Properties in Central New Mexico", University of California at San Diego, Scripps Institution of Oceanography, Visibility Laboratory, SIO Ref. 72-71, AFCRL-72-0461

- Duntley, S. Q., R. W. Johnson, and J. I. Gordon (1972), "Airborne Measurements of Optical Atmospheric Properties, Summary and Review", University of California at San Diego, Scripps Institution of Oceanography, Visibility Laboratory, SIO Ref. 72-82, AFCRL-72-0593.

- Duntley, S. Q., R. W. Johnson, and J. I. Gordon (1973), "Airborne Measurements of Optical Atmospheric Properties in Southern Illinois", University of California at San Diego, Scripps Institution of Oceanography, Visibility Laboratory, SIO Ref. 73-24, AFCRL-TR-73-0422.

- Duntley, S. Q., R. W. Johnson, and J. I. Gordon (1974), "Airborne and Ground-Based Measurements of Optical Atmospheric Properties in Southern Illinois", University of California at San Diego, Scripps Institution of Oceanography, Visibility Laboratory, SIO Ref. 74-25, AFCRL-TR-74-0298.

- Duntley, S. Q., R. W. Johnson, and J. I. Gordon (1975), "Airborne Measurements of Optical Atmospheric Properties in Western Washington", University of California at San Diego, Scripps Institution of Oceanography, Visibility Laboratory, SIO Ref. 75-24, AFCRL-TR-75-0414.

- Duntley, S. Q., R. W. Johnson, and J. I. Gordon (1975), "Airborne Measurements of Optical Atmospheric Properties, Summary and Review II", University of California at San Diego, Scripps Institution of Oceanography, Visibility Laboratory, SIO Ref. 75-26, AFCRL-TR-75-0457.

- Duntley, S. Q., R. W. Johnson, and J. I. Gordon (1976), "Airborne Measurements of Optical Atmospheric Properties in Northern Germany", University of California at San Diego, Scripps Institution of Oceanography, Visibility Laboratory, SIO Ref. 76-17, AFGL-TR-76-0188.

- Duntley, S. Q., R. W. Johnson, and J. I. Gordon (1977), "Airborne Measurements of Atmospheric Volume Scattering Coefficients in Northern Europe, Spring 1976", University of California at San Diego, Scripps Institution of Oceanography, Visibility Laboratory, SIO Ref. 77-8, AFGL-TR-77-0078.

- Duntley, S. Q., R. W. Johnson, and J. I. Gordon (1978), "Airborne Measurements of Atmospheric Volume Scattering Coefficients in Northern Europe, Fall 1976", University of California at San Diego, Scripps Institution of Oceanography, Visibility Laboratory, SIO Ref. 78-3, AFGL-TR-77-0239.

- Duntley, S. Q., R. W. Johnson, and J. I. Gordon (1978), "Airborne Measurements of Atmospheric Volume Scattering Coefficients in Northern Europe, Summer 1977", University of California at San Diego, Scripps Institution of Oceanography, Visibility Laboratory, SIO Ref. 78-28, AFGL-TR-78-0168.

- Duntley, S. Q., R. W. Johnson, and J. I. Gordon (1978), "Airborne Measurements of Optical Atmospheric Properties, Summary and Review III", University of California at San Diego, Scripps Institution of Oceanography, Visibility Laboratory, SIO Ref. 79-5, AFGL-TR-78-0286.
- Fitch, B. W. (1981), "Effects of Reflection by Natural Surfaces on the Radiation Emerging from the Top of the Earth's Atmosphere", to appear in *J. Atmos. Sci.* December 1981.
- Fitch, B. W. and T. S. Cress (1981), "Measurements of Aerosol Size Distributions in the Lower Troposphere over Northern Europe", to appear in *J. Appl. Meteor.*, Oct 1981.
- Gordon, J. I., J. L. Harris, Sr., and S. Q. Duntley (1973), "Measuring Earth-to-Space Contrast Transmittance from Ground Stations", *Appl. Opt.* 12, 1317-1324.
- Gordon, J. I., C. F. Edgerton, and S. Q. Duntley (1975), "Signal-Light Nomogram", *J. Opt. Soc. Am.* 65, 111-118.
- Gordon, J. I., (1979), "Daytime Visibility, A Conceptual Review", University of California at San Diego, Scripps Institution of Oceanography, Visibility Laboratory, SIO Ref. 80-1, AFGL-TR-79-0257.
- Hering, W. S. (1981), "An Operational Technique for Estimating Visible Spectrum Contrast Transmittance", University of California at San Diego, Scripps Institution of Oceanography, Visibility Laboratory, SIO Ref. 82-1, AFGL-TR-81-0198.
- Johnson, R. W., and J. I. Gordon (1979), "Airborne Measurements of Atmospheric Volume Scattering Coefficients in Northern Europe, Winter 1978", University of California at San Diego, Scripps Institution of Oceanography, Visibility Laboratory, SIO Ref. 79-25, AFGL-TR-79-0159.
- Johnson, R. W., W. S. Hering, J. I. Gordon, B. W. Fitch, and J. E. Shields (1979), "Preliminary Analysis & Modelling Based Upon Project OPAQUE Profile and Surface Data", University of California at San Diego, Scripps Institution of Oceanography, Visibility Laboratory, SIO Ref. 80-5, AFGL-TR-79-0285.
- Johnson, R. W. and J. I. Gordon (1980), "Airborne Measurements of Atmospheric Volume Scattering Coefficients in Northern Europe, Summer 1978", University of California at San Diego, Scripps Institution of Oceanography, Visibility Laboratory, SIO Ref. 80-20, AFGL-TR-80-0207.
- Johnson, R. W. (1981a), "Winter and Summer Measurements of European Very Low Altitude Volume Scattering Coefficients", University of California at San Diego, Scripps Institution of Oceanography, Visibility Laboratory, SIO Ref. 81-26, AFGL-TR-81-0154.
- Johnson, R. W. (1981b), "Daytime Visibility and Nephelometer Measurements Related to its Determination", *Atmospheric Environment* 15, Oct 1981, pp 1835.
- Johnson, R. W. (1981c), "Spring and Fall Measurements of European Very Low Altitude Volume Scattering Coefficients", University of California at San Diego,

Scripps Institution of Oceanography, Visibility Laboratory, SIO Ref. 81-33, AFGL-TR-81-0237.

APPENDIX B

Analytic Update

As noted in the text of the report, this analysis is based on preliminary release data issued by the Netherlands. More recently, an improved data base (coded "issue 5") has become available. The relative humidity values during fog have been readjusted from 94% to about 99% in the revised data base. The problem with the relative humidities discussed on p. 6 of this report (last paragraph) has been attributed to incorrect maintenance, and the values should be close to 100%, as suspected. This change in the data base would lead to a higher threshold value than the value of 94% given on p. 10 of this report, but would not otherwise affect the conclusions.

The plots on p. 8 show the error bar associated with $\pm 20\%$ uncertainty in scattering coefficient ($\pm 20\%$ of the measured value). As discussed on p. 4, this was the desired accuracy to be achieved by all stations (see Renn (1978)). More currently, the Netherlands assesses the ALG accuracy to be about $\pm 10\%$ (perhaps $\pm .0\%$ of full scale).

The discussion of persistence calculations, p. 19, notes that the autocorrelation $\rho(r)$ is expected to decay exponentially, in the absence of periodic variations. It should be noted that periodic variations do occur in these data, as shown in Janssen and van Schie (1982), however, the observed period is much too long (24 hours) to affect the analysis period (about 1 hour) in this report. Systematic variations of shorter period may in fact occur; this is one of the subjects undergoing current investigation.

It may be noted that the use of the definition "visibility $\equiv 3/S$ " on p. 10 is consistent with the term "visibility" used by McIntosh (1963) in the definition of mist repeated on p. 10. McIntosh states that "the World Meteorological Organization has recommended the use of the [contrast threshold] value .05, and this figure should be used for the purposes of conversion of attenuation measurements to corresponding visibility." The relation $V = 3/S$ is derived using a contrast threshold .05.

APPENDIX C

Further Comments on Infrared Aerosol Extinction Uncertainties

Section 5.2 discusses four sources of uncertainty which had to be considered in analyzing the data: the measurement uncertainty, the uncertainty due to non-simultaneity of the data, the uncertainty associated with the calibration procedure, and the uncertainty resulting from the molecular extinction. This appendix contains additional remarks on the interpretation of these uncertainties.

The first of the four uncertainties, measurement uncertainty, is due to detector noise, turbulence, and other such measurement problems. Detector noise and turbulence may be expected to yield random errors, however systematic errors, both known and unknown, may exist. The magnitude of the total uncertainty is difficult to assess. The goal was to achieve $\pm 2\%$. Some error sources tend to result in a constant ΔT , and others tend to result in a constant $\Delta T/T$. The actual error should be a fairly complicated function. See, for example, Douglas *et al.* (1977).^{*} We have used $\Delta T \approx 2\%$ in order to generate the error bars in Fig. 5-4. Note that since $T=e^{-\alpha r}$, we have $(dT/d\alpha)=-rT$, so

$$\frac{\Delta \alpha}{\alpha} = -\frac{1}{r\alpha} \frac{\Delta T}{T}$$

Thus if we assume constant ΔT , $\Delta \alpha/\alpha$ is smallest mid-scale on the transmissometer. The error bars for $\Delta \alpha/\alpha$ become large for T near 100% because α is small, and become large for T near 0%, because T is small, as shown in Fig. 5-4. On the other hand, if we assume constant $\Delta T/T$, then $\Delta \alpha/\alpha$ is large only for small α . Thus, if we had used $\Delta T/T \approx 2\%$ rather than $\Delta T = 2\%$, the error bars at low α in Fig. 5-4 would be essentially unchanged, but the error bars at high α would be smaller.

It should also be noted that Table 5.1, "Aerosol Extinction Uncertainty for $\pm 2\%$ Uncertainty in Total Transmittance", does *not* imply that we attribute the measurement error to variations in aerosol extinction. What it shows is, given an error in measured transmittance due to noise and other sources, there is a resulting error in the

aerosol extinction *computed* from that transmittance. The error in the computed extinction is illustrated in Fig. 5-4.

The second of the four uncertainties, the uncertainty due to non-simultaneity of the data, is not a measurement error. It is simply a complicating factor in the interpretation of plots such as Fig. 5-4. The fact that the measurements are not exactly simultaneous adds some uncertainty to our ability to interpret these plots. Section 5.2 discusses the magnitude of the time instability which causes this.

The third of the four uncertainties, the uncertainty associated with the calibration procedure, is a systematic error in the transmittances. As explained in Section 5.2, if the calibration measurements were noise free, the calibration constant would be exact, at least to the extent that Lowtran matches truth. However there is noise during the calibration measurement, so the calibration constant has a resulting small uncertainty. This uncertainty in the calibration constant results in a systematic error in the transmittances. This uncertainty should be small compared to the $\pm 2\%$ mentioned before.

The fourth of the four uncertainties is the uncertainty due to the molecular extinction calculation. In computing the aerosol extinction, it is necessary to extract molecular and water vapor extinction. If temperature and relative humidity are not precisely known, the computed molecular extinction will have an uncertainty, and therefore the computed aerosol extinction will have an uncertainty. Note that this is *not* a measurement uncertainty in the infrared transmittance, in fact the transmittance is unaffected by this. It is only the final computed aerosol extinction which is affected.

^{*}Douglas, C.A. and R.L. Booker (1977), "Visual Range: Concepts, Instrumental Determination, and Aviation Applications" U.S. Dept. of Transportation Report No. FAA-RD-77-8.